# Modeling and simulation of a biomass pyrolysis and gasification process

**Matheus Bonifacio**

Final dissertation report submitted to **Escola Superior de Tecnologia e Gestão** of **Instituto Politécnico de Bragança** to obtain the master's Degree in Chemical Engineering in the scope of the double diploma with the **Universidade Tecnológica Federal do Paraná.**

Supervisors:

**Prof. Paulo Miguel Pereira de Brito**

**Prof. Helder Teixeira Gomes**

**Prof. Admilson Lopes Vieira**

Bragança

February, 2023

This page was intentionally left blank.

# Acknowledgements

I would like to thank above all my parents, if I got this far it was because I always had the support I needed. I would like to thank my family members who participated in my journey, and I am sure they will continue to support me. I would like to thank my advisors, Prof. Paulo Miguel Pereira de Brito, Prof. Helder Teixeira Gomes, and co-advisor Prof. Admilson Lopes Vieira for all the guidance and help during the development of this work. I would like to thank Prof. Patricia Yassue Cordeiro for their friendship and guidance throughout my course. I thank all my colleagues who participated in my journey, if it were not for them, I would not have gotten this far, especially to my friends Vitor Barbieeri and Ana Paula Silva Natal for all the work done together, and Raul Dias, who on several occasions was the teacher I needed. Thank you all for all the affection and love, I did not mention all the names, but everyone who helped me knows how grateful I am. Finally, I thank UTFPR for providing a quality public education, and for the IPB for the opportunity and the means to carry out my work.

# Abstract

Global energy demand has increased exponentially, and the trend is to continue to increase. The form of conventional energy production, primarily from fossil and non-renewable energies, is very harmful to the planet. Biomass is a good alternative to fossil energies due to being renewable and possessing virtually no production of carbon dioxide, one of the main gases that cause the greenhouse effect. There are several ways to use biomass, it should be mentioned: pyrolysis, gasification for fuel production, direct burning, bio digestion and others. The objective is to review the generation of waste in Portugal, present the classic models of pyrolysis and biomass gasification as well as their stages, and later develop a specific model for the simulation of a downdraft due to the high temperature selected gasifier process using Python and the UniSim Design chemical processes simulator software. The study was made using two different sources of biomass, olive pit and wood residue. A kinetic and thermodynamic model was developed to first evaluate the pyrolysis process, and using the software Unisim Design a gasification process was developed. The main results obtained allow the conclusion that the biomass with higher moisture content (wood residue) was more susceptible to temperature influence in the process than the biomass with lower moisture content (olive pit), leading to the formation of compositions for $H_2$ of approximately 0.246 (mass fraction) between 100 and 400 °C for olive pit and 0.106 and 0.0105 (mass fraction) for wood residue between 100 and 400 °C, in stoichiometric equivalence between biomass, steam and water. Olive pit generated higher hydrogen and methane formation. Increasing the temperature and steam inlet favors the formation of $H_2$, CO and $CO_2$ while decreasing $CH_4$ formation, $H_2$ obtained a variation of 0.250 to 0.234 (mass fraction) for olive pit and 0.106 and 0.103 (mass fraction) for wood residing in a biomass/steam molar equivalence between 0.5 and 4. Increasing the steam flow results in increased formation of $CO_2$ and $H_2$, and increased airflow decreases the formation of these products. The increase in steam flow decreases the formation of $CH_4$ and CO. Steam temperature of 250°C is the one with the highest hydrogen yield, and lower methane formation.

**Keywords:** Biomass; gasification; pyrolysis; Unisim Design software; simulation.

# Resumo

A demanda global de energia aumentou exponencialmente, e a tendência é continuar a aumentar. A forma de produção de energia convencional, principalmente a partir de energias fósseis e não renováveis, é muito prejudicial ao planeta. A biomassa é uma boa alternativa às energias fósseis por ser renovável e não possuir praticamente nenhuma produção de dióxido de carbono, um dos principais gases causadores do efeito estufa. Existem várias maneiras de usar a biomassa, deve-se mencionar: pirólise, gaseificação para produção de combustível, queima direta, biodigestão e outros. O objetivo é rever a geração de resíduos em Portugal, apresentar os modelos clássicos de pirólise e gaseificação de biomassa, bem como as suas fases, e posteriormente desenvolver um modelo específico para a simulação de um processo de gaseificador de corrente descendente utilizando Python e o software simulador de processos químicos UniSim Design. O estudo foi feito usando duas fontes diferentes de biomassa, caroço de azeitona e resíduo de madeira. Um modelo cinético e termodinâmico foi desenvolvido para primeiro avaliar o processo de pirólise, e usando o software Unisim Design um processo de gaseificação foi desenvolvido. Os principais resultados obtidos permitem concluir que a biomassa com maior teor de umidade (resíduo de madeira) foi mais suscetível à influência da temperatura no processo do que a biomassa com menor teor de umidade (azeitona), levando à formação de composições para $H_2$ de aproximadamente 0,246 (fracção mássica) entre 100 e 400 °C para a caroço oleícola e 0,106 e 0,0105 (fracção mássica) para o resíduo de madeira entre 100 e 400 °C, em equivalência estequiométrica entre biomassa, vapor e água. A fossa de azeitona gerou maior formação de hidrogênio e metano. O aumento da temperatura e da entrada de vapor favorece a formação de $H_2$, CO e $CO_2$ enquanto diminui a formação de $CH_4$, $H_2$ obteve uma variação de 0,250 a 0,234 (fração mássica) para caroço de azeitona e 0,106 e 0,103 (fração mássica) para a resíduo de madeira em uma equivalência molar biomassa/vapor entre 0,5 e 4. O aumento do fluxo de vapor resulta no aumento da formação de $CO_2$ e $H_2$, e o aumento do fluxo de ar diminui a formação desses produtos. O aumento do fluxo de vapor diminui a formação de $CH_4$ e CO. A temperatura de vapor de 250 °C é a que tem o maior rendimento de hidrogênio e menor formação de metano.

**Descritores:** Biomassa; gaseificação; pirólise; software Unisim Design; simulação.

# TABLE OF CONTENTS

## LIST OF FIGURES

## LIST OF TABLES



## LIST OF APPENDIXES

## LIST OF ACRONYMS

VM – Volatile matter

W – Humidity

FC – Fixed carbon

HHV – Higher heating value (kJ/g)

LHV – Lower heat value (kJ/g)

$\Delta H°$ - Enthalpy variation (kJ/kg)

$\Delta U°$ - Internal energy variation (kJ/kg)

Cb – Concentration of biomass

$C_{C1}$ – Concentration of solids 1 (mass fraction)

$C_{C2}$ – Concentration of solids 2 (mass fraction)

$C_{G1}$ – Concentration of volatiles 1 (mass fraction)

$C_{G2}$ – Concentration of volatiles 2 (mass fraction)

yi – mass fraction of component i

HR – Heating rate (K/s)

T – Temperature (K)

Char – Charcoal

Tar – Liquids

t – Time (s)

# *Part 1 - Introduction*

Global energy demand has increased exponentially, and the trend is to continue to increase. The form of conventional energy production, primarily from fossil and non-renewable energies, is very harmful to the planet. Over the years, sustainable thinking has become indispensable to prevent environmental pollution. In this context, more and more renewable energies are emerging as an option, such as solar energy, wind energy, or the production of renewable fuels, such as biomass (Funabashi, 2016).

Biomass is a good alternative to fossil energies due to being renewable and possessing virtually no production of carbon dioxide, one of the main gases that cause the greenhouse effect, during plant growth is consumed carbon dioxide that will be generated during burning. Biomass can be generated by organic matter, such as wood products, sugarcane bagasse, dry vegetation, food husks, aquatic plants, and even organic residues (Funabashi, 2016). There are several ways to use biomass, it should be mentioned: pyrolysis, gasification for fuel production, direct burning, bio digestion and physical-chemical conversion. This work will mainly address the treatment of pyrolysis and gasification (Andrade, 2007).

The main routes for the conversion of lignocellulosic biomass into biofuels are applied, the biochemical route that uses a pre-treatment of hydrolysis and subsequent fermentation and the thermochemical route through pyrolysis and gasification that generates a synthesis gas to be carried out a catalytic synthesis or fermentation, thus generating hydrocarbons, ammonia, hydrogen, and synthetic natural gas (Vieira et al., 2014).

Pyrolysis is a thermochemical degradation process that occurs when too much heat is applied to a material or substance in the total absence of oxidant, some processes allow a small amount of oxidant. Being an endothermic process, an external source is needed that provides energy, the products of this process can be solid, gaseous, or liquid. The solid fraction basically consists of carbon ash that can be used as fuel or in the manufacture of activated carbon. The liquid fraction is a complex mixture of oxygenated aromatic and aliphatic components, having a high energy value, these oils can be used in combustion chambers and diesel engines. The gas fraction is also combustible, consisting of CO, $CO_2$, $H_2$, $CH_4$ and other hydrocarbons (Andrade, 2007).

Gasification on the other hand is the thermochemical conversion process of a solid or liquid material, which contains carbon in its composition, in a fuel, through partial

oxidation at high temperatures and atmospheric pressure or higher. A gasification agent is used, which may be air, water vapor, oxygen, or a mixture of these, in amounts lower than combustion stoichiometry. This process generates fuels such as CO, $H_2$, $CH_4$ and in smaller quantities is also generated, $CO_2$, $H_2O$ and $N_2$, and lower levels of hydrocarbons such as ethene and ethane (Barriquelo, 2013).

The last two processes presented are a good alternative to increase the energy potential of biomass, the most usual process is only burning, however using the pyrolysis and gasification process it is possible to transform these residues into fuels, being more easily used and thus increasing their profitability.

## 1.1 General Objective

In this context, the objective is to review the generation of waste in Portugal, present the classic models of pyrolysis and biomass gasification as well as their stages, and later develop a specific model for the pyrolysis products formation prediction using Python and simulation of a downdraft gasification process using the UniSim Design chemical processes simulator software.

## 1.2 Economic analysis

Among the possible sources of biomass, it is worth mentioning the forest waste, woody from exploration, management, and installation, which is the biomass most easily used for energy conversion. Cunha and Marques (2019) collected data that the forests of Portugal produce about 9.3 million tons of primary forest biomass, of these only 763 thousand tons can be accounted for energy production, since the others are used to supply the national industry (sawmill, pulp, and others).

Also in the study by Cunha and Marques (2019) a survey of approximately 2 million tons/year is obtained from forest residues, unlike the study surveyed by the government itself, presented in the "Plano Nacional de Biorrefinarias" (RCM No. 163/2017) where the amount presented was 1.5 million tons per year, also inclusive in the residual biomass for entry  is arbor biomass where there are not many studies available to

carry out such a survey, however, SPC No. 163/2017 points to about 1 million tons per year.

Finally, on residual forest biomass, there is waste from industry, about 5.3 million tons/year. All these forest residues have great energy value and can be used both in the burning process (the most usual process), as well as in more sophisticated processes with higher energy value, such as the gasification or pyrolysis process. A good example of using more sophisticated processes to produce fuels from waste is addressed in the action plan for waste management of the company "Resíduos do Nordeste" that addresses among the various strategies for the treatment of waste gasification, reaffirming once again the feasibility of such a process.

## 1.3 Layout

To carry out the study, the work is divided into five parts. In the first part (Part 1 – Introduction) is presented the contextualization, motivation, and objectives of the work, as well as presenting biomass and its importance as a fuel. In the second stage (Part 2 – State of the art) is presented a more in-depth study on the composition of biomass, the conversion processes and the simulation models currently used, as well as the tools applied (software) which are also presented. In the third stage (Part 3 - Methodology) is described the simulated process, as well as the considerations and development of the study, and there are also shown the process flow diagrams and the taken steps are described. In the fourth part (Part 4 - Results and discussion) the results obtained in each of the stages are commented and compared with the results available in selected relevant literature. In the last part (Part 5 – Conclusion and future works) are presented the conclusions obtained and a few suggestions of future work.

# *Part 2 - State of the art*

## 2.1 Biomass

First, it is necessary to define what is meant by biomass and what will be considered in this work, since this is a very broad term. The definition to be used is that presented by the United Nations Framework Convention on Climate Change (UNFCCC, 2005):

"Biomass means non-fossilized and biodegradable organic matter from plants, animals and microorganisms. This should also include products, by-products, waste and waste from agriculture, forestry, and related industries, as well as the non-fossilized and biodegradable fractions of industrial and municipal waste. Biomass also includes gases and liquids recovered from the decomposition of non-fossilized and biodegradable organic matter."

The definition presented is quite broad, being considered as biomass a vast amount of material, in subsequent topics will be addressed the different types of biomasses and its composition.

### 2.1.1 Immediate composition

The immediate composition allows studying the contents of moisture, ash, volatile materials and fixed carbon present in biomass, the annual crops of fast growth have higher moisture and ash content compared to stems, bark trunks and tree branches.

#### *2.1.1.1 Humidity*

The definition of moisture content in biomass is the amount of free water in the material, although some types of wood can have humidity of up to 80% generally, for the most common types of biomasses, this content remains between 3 and 63% depending also on its type of storage. Another definition is an aqueous solution containing mineralized cations ($Al^{3+}$, $Ca^{2+}$, $Fe^{3+}$, $K^{+}$, $Mg^{2+}$, $Mn^{2+}$, $Na^{+}$, $Ti^{4+}$), anions ($Br^{-}$, $Cl^{-}$, $CO_3^{2-}$, $F^{-}$, $HCO_3^{-}$, $H_2PO_4^{-}$, $I^{-}$, $NO_3^{-}$, $OH^{-}$, $PO_4^{3-}$, $SO_4^{2-}$) (Vassilev et al., 2010).

The amount of moisture has an influence on the process of energy conversion, with the increase of humidity the calorific potential value of the fuel produced from biomass is decreased with the increase of moisture, this is due to the high convective coefficient of water (Loo, 2008).

#### *2.1.1.2 Ashes*

The determination of the ash content is performed between 550 and 600 ºC, and for the most common types of biomasses varies between 0.1 and 46%. At high temperatures the ash contents affect thermochemical conversion processes to produce the formation of slag and agglomerations, thereby increasing the maintenance costs of the equipment, increasing the overall cost of the process as a result. The most common elements found in biomass ash are Si, Al, Fe, Ca, Mg, Na, K, S and P (Vassilev et al., 2010).

#### *2.1.1.3 Volatile material*

The volatile content is defined as the fraction released when it is heated to 900 ºC in inert atmosphere. In the process of volatilization biomass is decomposed into volatile materials, such as: tars, volatile gases, CO, $CO_2$, $H_2$. The volatile matter content in biomass is high, indicating that this fuel is easy to ignite, the content varies between 48 and 86% (Quaak et al., 1999; Vassilev et al., 2010).

#### *2.1.1.4 Fixed carbon*

Finally, fixed carbon is the mass fraction that is maintained after the release of all volatiles, excluding ash and moisture content. Biomass generally has a fixed volatile/carbon ratio greater than 3.5 (McKendry, 2002a).

### 2.1.2 Elemental composition

The main elements present in the composition of biomass are carbon, hydrogen, and oxygen, as well as in fossil fuels these elements are more present due to the high content of hydrocarbons representing about 45% of dry matter. The high oxygen content is very interesting for the creation of fuels because it provides better combustion with lower oxygen demand. Other elements present, in smaller quantities, are nitrogen, sulfur and chlorine, these are responsible for pollutant emissions and the smaller the amount of these in biomass, the better the fuel obtained, are also found in small quantities other elements, but due to the fact that they do not significantly influence the calorific value and/or environmental factor, except for some different cases, will not be addressed in this study (Ferreira, 2013).

The elemental composition allows the determination of the calorific power and the needs of adding comburent to the process. Moisture and ash have great influence on the conversion process, because of this, comparative characterizations of the various types of this resource are performed through elemental analysis and chlorine content (Khan et al., 2008).

#### *2.1.2.1 Carbon, oxygen, and hydrogen*

In biomass the total carbon content varies between 42-71%. High carbon content is mainly observed in forest residues such as wood shells, also in ash residues, and meat and bone meal. The oxygen content in biomass is higher in pepper, coffee, and soybean hull residues, ranging from 16 to 49%. The hydrogen content in biomass is usually between 3-11%. A higher hydrogen content in biomass is observed in forest residues such as pine bark, mustard bark, cotton, meat, and bone meal derived from fuel and peanut shells (Vassilev et al., 2010).

*2.1.2.4 Nitrogen, sulfur, and chlorine*

Nitrogen, in large quantities, is harmful to plant growth, however it exists in different types of biomasses in small amounts, so its content varies between 0.01-12%. The high nitrogen content is mainly observed in meat and bone meal, chicken bed residues, sewage sludge, pepper residues and palm seed the sulfur content of biomass varies from 0.01 to 2.3%, the highest sulfur content is observed mainly in mixed biomass, pepper residues, sewage sludge, chicken bed residues, waste derived from fuel and pine.

The chlorine content in biomass is usually the lowest, studies indicate that this content varies between 0.01-0.9%, the order of chlorine is like that of nitrogen and sulfur, possibly indicating its association in salts, the high content of chlorine is observed in waste derivatives, meat and bone meal, corn, barley, mint, rice, and wheat. On the other hand, most wood residues have a very low chlorine content if they do not contain chlorine additives (Vassilev *et al.*, 2010; Ferreira, 2013).

*2.1.2.5 General table of immediate and elementary composition*

The following is the table of immediate and elementary composition of different types of biomasses studied by different authors (see Table 1).

Table 1 - General table of immediate and elementary composition.

| Type of biomass | VM (%) | FC (%) | W (%) | Ashes (%) | C (%) | O (%) | H (%) | N (%) | S (%) | Reference |
|---|---|---|---|---|---|---|---|---|---|---|
| Eucalyptus bark | 68.7 | 15.1 | 12.0 | 4.2 | 48.7 | 45.3 | 5.7 | 0.3 | 0.05 | Theis *et al*. (2006) |
| Forest residue | 34.5 | 7.3 | 56.8 | 1.4 | 52.7 | 41.1 | 5.4 | 0.7 | 0.1 | Miles *et al*. (1995) |
| Oak sawdust | 76.3 | 11.9 | 11.5 | 0.3 | 50.1 | 43.9 | 5.9 | 0.1 | 0.01 | Miles *et al*. (1995) |
| Oak wood | 73.0 | 20.0 | 6.5 | 0.5 | 50.6 | 42.9 | 6.1 | 0.3 | 0.1 | Demirbas, A. (2004) |
| Olive wood | 74.3 | 16.1 | 6.6 | 3.0 | 49.0 | 44.9 | 5.4 | 0.7 | 0.03 | Vamvuka and Zografos. (2004) |
| Pine bark | 70.2 | 23.3 | 4.7 | 1.8 | 53.8 | 39.9 | 5.9 | 0.3 | 0.07 | Bryers (1996) |
| Wood | 77.5 | 14.5 | 7.8 | 0.2 | 49.6 | 44.1 | 6.1 | 0.1 | 0.06 | Wei, Schnell, Hein. (2005) |
| Wood residue | 57.4 | 12.2 | 26.4 | 4.0 | 51.4 | 41.9 | 6.1 | 0.5 | 0.08 | Miles *et al*. (1995) |
| Grass | 46.5 | 9.5 | 42.0 | 2.0 | 48.7 | 44.5 | 6.1 | 0.6 | 0.13 | Miles *et al*. (1995) |
| Banana grass | 70.2 | 15.9 | 4.5 | 9.4 | 50.1 | 42.9 | 6.0 | 0.9 | 0.13 | Miles *et al*. (1995) |
| Alfalfa straw | 71.6 | 14.3 | 9.3 | 4.8 | 49.9 | 40.8 | 6.3 | 2.8 | 0.21 | Miles *et al*. (1995) |
| Corn straw | 67.7 | 17.8 | 7.4 | 7.1 | 48.7 | 44.1 | 6.4 | 0.7 | 0.08 | Masia et al. (2007) |
| Rice straw | 59.4 | 14.4 | 7.6 | 18.6 | 50.0 | 43.0 | 5.7 | 1.0 | 0.16 | Miles *et al*. (1995) |
| Wheat straw | 67.2 | 16.3 | 10.1 | 6.4 | 49.4 | 43.6 | 6.1 | 0.7 | 0.17 | Demirbas (2004) |
| Mustard peel | 68.5 | 22.0 | 5.6 | 3.9 | 45.8 | 44.4 | 9.2 | 0.4 | 0.2 | Werther (2000) |
| Olive peel | 73.7 | 17.4 | 6.8 | 2.1 | 50 | 42.1 | 6.2 | 1.6 | 0.05 | Demirbas (2004) |
| Olive pit | 72.3 | 18.7 | 6.1 | 2.9 | 52.8 | 39.4 | 6.6 | 1.1 | 0.07 | Vamvuka and Zografos. (2004) |
| Rice husk | 56.1 | 17.2 | 10.6 | 16.1 | 49.3 | 43.7 | 6.1 | 0.8 | 0.08 | Miles *et al*. (1995) |
| Municipal solid waste | 50.9 | 18.8 | 7.6 | 22.7 | 36.4 | 5.0 | 10.1 | 1.4 | 0.8 | Ramzan *et al* (2011) |

### 2.1.3 Composition of organic and inorganic matter

Biomass has great variability in its composition since it has different levels of ash, moisture, and genetic types of matter. The origin of biomass, storage and treatment strongly impacts on its composition, and the moisture content can reach 80% and ash production can reach 46% (Ferreira, 2013).

#### *2.1.3.1 Organic matter*

The organic part of the biomass has in its composition three main polymers: cellulose, hemicellulose, and lignin. Cellulose is the most abundant natural polymer on earth, secondly, representing about 30% of all non-fossil organic carbon is lignin. In forest or plant residues, the presence of polymers such as cellulose (Laurichesse and Avérous, 2014).

#### *2.1.3.2 Soluble matter*

The soluble matter of biomass is represented by a set of ions of complex origin soluble in water, such residues can be obtained from detritus or organic residues. The soluble part of biomass usually varies between 10 and 60% and can, in rare cases, reach 80% (Laurichesse and Avérous, 2014).

#### *2.1.3.3 Inorganic matter*

A large part of the biomass is represented by inorganic matter, this part includes mineral matter, namely mineral and mineraloid species poorly crystallized from different groups of minerals, as well as amorphous inorganic phases of detritic and anthropogenic origin (Ferreira, 2013).

### 2.1.4 Energy content

The energy evaluation of fuels is carried out from the determination of calorific value. For the design of a fuel producing plant this parameter is extremely important. In this study, the identification of this parameter is extremely important since the objective is the production of a fuel.

The calorific value is defined as the amount of heat supplied to the outside when a certain amount (mass or volume) of matter is burned in a calorimeter under pressure or constant volume conditions, defining itself as enthalpy and internal energy respectively and having as liquid or gaseous product water (Matos, 2008). The following is a table relating the concepts presented.

Table 2 - Thermodynamic differences between HHV and LHV, adapted from Matos, (2008).

| Calorific power | | Thermodynamic equation | Physical state of water |
|---|---|---|---|
| HHV | Constant volume | $HHVv = \Delta U°_{comb,water(l)}$ | Liquid |
| | Constant pressure | $HHVp = \Delta H°_{comb,water(l)}$ | |
| LHV | Constant volume | $LHVv = \Delta U°_{comb,water(g)}$ | Gaseous |
| | Constant pressure | $LHVp = \Delta H°_{comb,water(g)}$ | |

Table 2 presented by Matos (2008) shows that calorific value is divided into two types: HHV (higher heating value) and LHV (lower heating value). The HHV corresponds to the amount of energy released in the complete combustion of a unit of mass, and water as a product in the case of biomass burning. This parameter is determined experimentally in the laboratory, this parameter is also studied in cases of fire prevention, and it is very useful in the prevention of forest fires (Regueira et al., 2001). The LHV differs from the HHV only in the physical state of the water formed during biomass combustion, while the HHV the water remains liquid, in the LHV a water is observed in the gaseous phase, and this variable can be determined from the HHV value of the same sample (Matos, 2008).

The calorific value of agricultural waste varies between 15 and 17 MJ/kg and forest residues have values between 18 and 21 MJ/kg, it is verified that biomass has a lower calorific value compared to fossil fuels (20-30 MJ/kg), so it is very interesting that

thermochemical conversion processes are carried out to produce biofuels from biomass thus performing the elevation of calorific value (Saião, 2009).

The moisture content has a great influence on the calorific value of biomass, which is inversely proportional, that is, the higher the moisture, the lower the calorific value. Calorific power is also influenced by carbon, hydrogen, and oxygen content, increasing with the greater presence of carbon and hydrogen, and decreasing with the presence of oxygen. The increase in the moisture content of biomass can also cause problems in treatment equipment because it has a higher chance of oxidation.

## 2.2 Biomass conversion

Biomass is widely used to produce liquid and gaseous solid fuels. Thermochemical conversion technologies are used for this, with emphasis on combustion, pyrolysis, and gasification. Figure 1 shows the main sources, conversion processes and the fuel obtained:

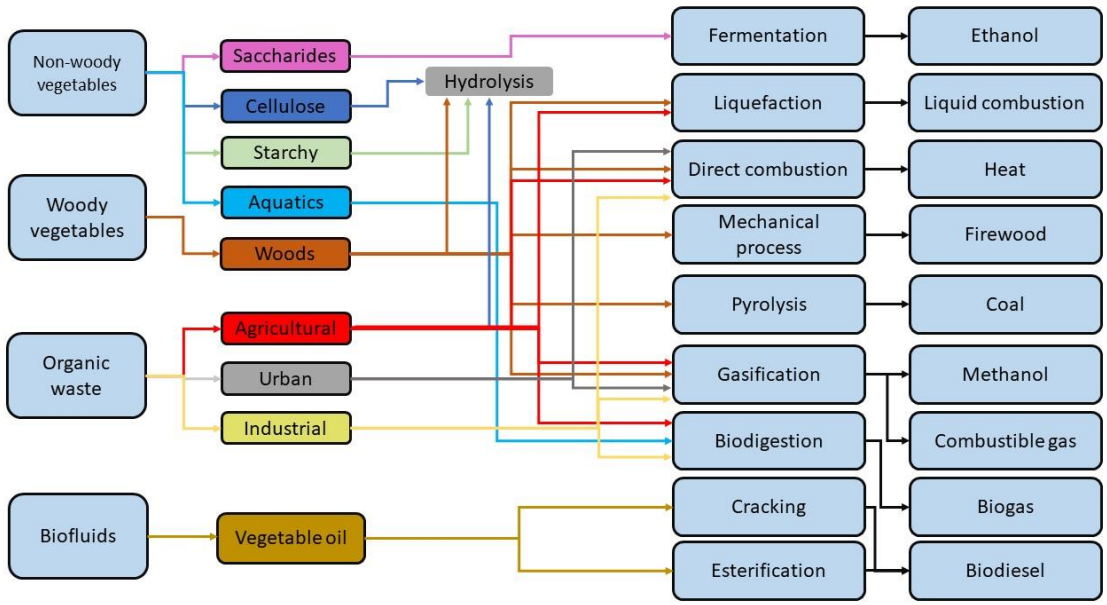


Figure 1 - Processes of conversion of biomass into fuels, adapted from ANEEL (2005).

From these processes are generated fuels such as bio-oil, gas, heat, or coal. To increase the efficiency of conversion processes, processes from the oldest to the most

current are studied, which are pyrolysis and gasification (Fernandes, 2012). This work will address the themes of gasification and pyrolysis.

### 2.2.1 Biomass gasification

Gasification is a thermochemical technology to change the structure of biomass at high temperatures in the presence of a gasification agent, resulting in a higher production of gaseous products and small amounts of coal, tar, and ash. The process can occur directly (using air or oxygen to produce heat) or indirectly (using an external heat source) (Rodrigues, 2019).

In the gasification process, biomass undergoes partial pyrolysis under sub stoichiometric conditions and with controlled air supply, usually 1.5 and 1.8 kg of air per kg of biomass are used. After this process, a mixture of gases composed of carbon monoxide (CO), hydrogen ($H_2$), carbon dioxide ($CO_2$), methane ($CH_4$) and water ($H_2O$) are obtained, in addition to tar, ash and other compounds that must be removed depending on the application (Rodrigues, 2019). The following are the steps of the gasification process:

#### *2.2.1.1 Drying*

Drying is the first process in the thermochemical conversion route by gasification. The purpose of this process is to reduce the moisture of the material, depending on the type of biomass the humidity may be higher or lower. At this stage there is evaporation of the water present in the biomass by adding heat in the combustion zone. The purpose of this process is to leave the biomass with a humidity below 2%, because the lower the humidity, as the particles move to the depollution and reduction zone, the higher the quality of the fuel. This process is endothermal and uses about 2400 kJ/kg for water (Aranda et al., 2016)

*2.2.1.2 Pyrolysis in aerator*

The gasification process first requires a pyrolysis process. This process is the thermochemical decomposition of biomass. Pyrolysis is the result of thermal transformation of biomass at a temperature below 600°C, through heat the original solid is decomposed into a mixture of solid (coal, carbon, and ash), liquid (tar, heavy hydrocarbons, and water) and gases ($CO_2$, $H_2O$, CO, $C_2H_2$, $C_2H_4$, $C_2H_6$, $C_6H_6$, etc.). The proportions of these products depend on the quality of biomass (Rodrigues, 2019).

*2.2.1.3 Combustion*

The combustion process is the reaction of the material with oxygen. This process is responsible for providing heat for the other stages of the process, and may occur in the reactor itself, in a combustion chamber or in a secondary heat generator. In this process is burned the solid and liquid part of the material, a part of the gases and even the primary fuel. Since biomass is rich in carbon this process results in $CO_2$ emissions, and if in stoichiometric quantities there is CO emission as well. The hydrogen available in biomass is also oxidized, resulting in water. This process, depending on the quality of biomass, can result in the production of sulfites and nitrites, gases causing acid rain. Oxidation reactions are exothermic and responsible for the supply of energy to the other subsequent endothermic processes in the aerator (Mahamulkar et al., 2016).

*2.2.1.4 Reduction*

The reduction occurs when carbon and hydrocarbons of the fuel react partially with oxygen, giving rise to fuels such as carbon monoxide (CO) and hydrogen ($H_2$), this reaction only occurs in low presence of oxygen, and occurs in the aerator reduction zone. At a temperature of 800–1000ºC and under a sub stoichiometric presence a series of oxidation/reduction reactions occur. The types of reactions that occur are: Boudouard reactions, water-gas reactions, displacement reactions and methane reactions, to be promoted by the proportion of synthesis gas or $CO/H_2$ desired for the aerator. For

hydrogen production, as for ammonia synthesis, application in fuel cells, CO displacement and reformed reaction of $CH_4$ under the presence of steam is aimed at the application of hydrogen (Janajreh et al, 2021).

### 2.2.2 Biomass pyrolysis

Similarly, to the process described above, there is the possibility of performing only pyrolysis and no subsequent process to obtain a solid fuel, since pyrolysis is a process that can be summarized as the decomposition of matter that occurs at high temperatures. The reaction can be described by the following equation:

$$\text{Dry biomass} + \text{Solid} \rightarrow \text{Coal}_{\text{heat}} + \text{Liquid tar} + \text{Gases}$$

These reactions are exothermic up to 300ºC, being endothermic for higher temperatures (Mesquita, 2017).

Pyrolysis is a very complex process due to its series of exothermic and endothermic reactions that occur simultaneously (Lisboa, 2016). As previously described, pyrolysis of biomass is a process in which fuel (biomass) is decomposed in the absence or almost absence of an oxidizing agent, in most cases the oxidizing agent is air. This phenomenon usually occurs at temperatures above 250 ºC, where larger molecules, for example hydrocarbons, decompose into smaller molecules (Castanheira, 2017).

In this process, three products are usually obtained: tars, gas and charcoal in quantities related to the method and parameter of operation. Rapid pyrolysis is used to maximize the production of liquid products and the slow pyrolysis is designed to increase solid fuel production (Lisbon, 2016). Figure 2 is a schematic representation of the various types of pyrolysis, with information about the typical temperatures and reaction times, and the products formed.

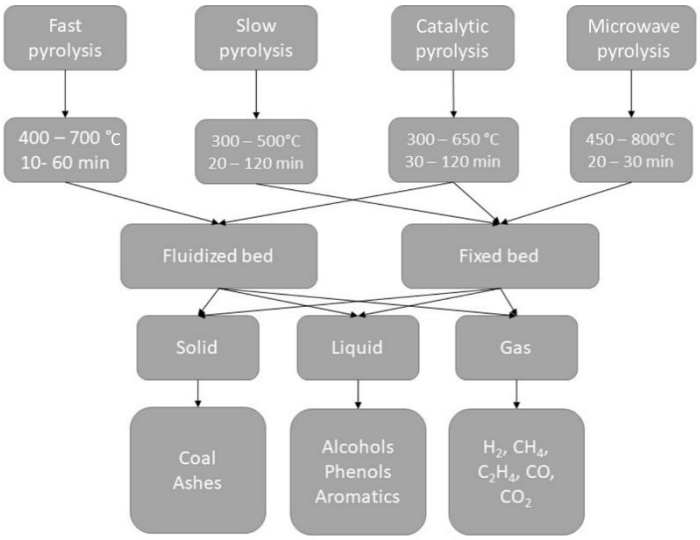


Figure 2 - Representation of the pyrolysis process, adapted from Das et al. (2021).

The three main steps in the pyrolysis process are: dehydration, devolatilization and decomposition. Dehydration occurs at temperatures below 200°C, while devolatilization occurs in the range of 220-550°C, and the final stage, decomposition, occurs at a temperature of 550°C. In pyrolysis the decomposition of carbohydrates and proteins occurs at temperatures below 400°C while lipid decomposition only occurs at temperatures above 550°C (Das et al., 2021). In subsequent topics will be explored the types of pyrolysis and their conditions of operation more in depth, being rapid pyrolysis, slow pyrolysis, catalytic pyrolysis, and microwave pyrolysis. In this study it is chosen the fast pyrolysis.

*2.2.2.1 Rapid pyrolysis*

The process begins by drying and grinding the biomass with a particle size of 1 mm or smaller before entering the reactor. Biomass is rapidly heated and decomposed into gases and molecules of smaller chain in the reactor and is cooled to produce liquid fuels. To maximize the production of liquid fuels biomass should be heated quickly and cooled quickly. This process occurs at high temperatures (400-700°C) and has a high yield for bio-oils (Das et al., 2021). The yield of the bio-oil produced from this process is a mixture of water and other organic compounds. The bio-oil obtained has a higher

content of oxygenated compounds and a much-reduced number of hydrocarbons. The global rapid pyrolysis process is an efficient and high-yield process, besides being fast (Sahoo et al., 2021; Maniscalco et al., 2020).

#### *2.2.2.2 Slow pyrolysis*

As its name suggests, slow pyrolysis, unlike rapid pyrolysis, occurs at a slower rate of heating and residence time. Because of this longer residence time there is an increase in bio coal and non-condensable gases such as $CO_2$, $H_2$, $CH_4$ and $C_2H$ 4, during the biomass conversion process, the reaction rate of this process is very slow. A preheating process is carried out to reduce the moisture content of biomass, then biomass is decomposed into lipids, carbohydrates and proteins that lead to the formation of charcoal, liquids, or gases. Finally, charcoal is decomposed into carbon-rich solid waste. This process is strongly influenced by temperature and residence time conditions, affecting the yield of biofuels. The main disadvantage of this process is their time of residence (Sahoo et al., 2021; Maniscalco et al., 2020).

#### *2.2.2.3 Catalytic pyrolysis*

The method of catalytic pyrolysis is based on adding a quantity of catalyst to the oil of rapid pyrolysis, this has a higher viscosity, lower heating value with higher oxygenated compounds and higher water content. The catalyst can break down the larger molecular compounds, making them lighter during the process. The process temperature is in the range of 300-500°C and the catalyst and biomass ratio are 0.2 to 5. According to Das et al. (2021), the catalytic pyrolysis process increased yield by 40% in terms of energy recovery (Das et al., 2021; Zhang et al. 2020).

#### *2.2.2.4 Microwave pyrolysis*

As its name suggests, microwave heating is carried out in this case. The electromagnetic rays that pass through the biomass generate the thermal energy necessary for the process, however the conventional method requires a heated external surface to heat the biomass (Zhang et. al. 2020). This method creates uniformity in biomass heating, which depends on two mechanisms, ionic conduction, and dipolar polarization. This process is very similar to the conventional process with the addition of a microwave oven. The oven is composed of quartz materials and borosilicate glass, the heating of this oven is different from normal because it depends on the power configuration of the oven and microwave absorption capabilities of biomass. In this process the temperature varies between 433 and 800°C, and the power of the oven varies between 500 and 2250 W. This energy process is efficient compared to other methods, it generates less ash and consumes less energy and reduces residence time by significantly increasing the yield of synthesis gas (Das et. al., 2021; Zhang et. Al. 2020).

## 2.3 Types of reactors in pyrolysis and biomass gasification

Over the years different pyrolysis and gasification technologies are developed, many of these technologies can be applied for pyrolysis and biomass gasification. In this topic will be showed the different technologies currently used in such process.

### 2.3.1 Gasification

The aerators used on an industrial scale generally differ by mode of contact between the feeding and the aerator agent, mode and heat transfer rate, time of residence of the material in the reaction zone. Depending on the plant demand, different technologies can be implemented, the mode of contact of biomass with the aerator agent can be concurrent, countercurrent or cross flow. Heat can be supplied externally or by a fuel directly inside the reactor. Residence time can vary between hours or minutes (McKendry, 2002c).

*2.3.1.1 Fixed-bed reactor*

The gasification process using a fixed bed reactor is the most traditional, usually operating at temperatures around 1000 °C. Fixed bed reactors can be classified into three types depending on the direction of the airflow: up flow, down flow, and cross flow.

**-Fixed bed reactor with ascending airflow:**

In this type of reactor, the airflow is introduced through the bottom of the aerator through a grate and the feed is introduced from the top. Immediately above the residual solid part goes into combustion, reaching a temperature of 1000°C, this is the residue that did not volatilized during the process (McKendry, 2002c). The ashes fall through the grate and the hot gases rise and are reduced. A little above in the aerator the biomass is pyrolyzed, and in the upper zone the feed is dry, cooling the gases to about 300°C (Molino, et al., 2016). Figure 3 demonstrates a fixed-bed upstream airflow reactor scheme.

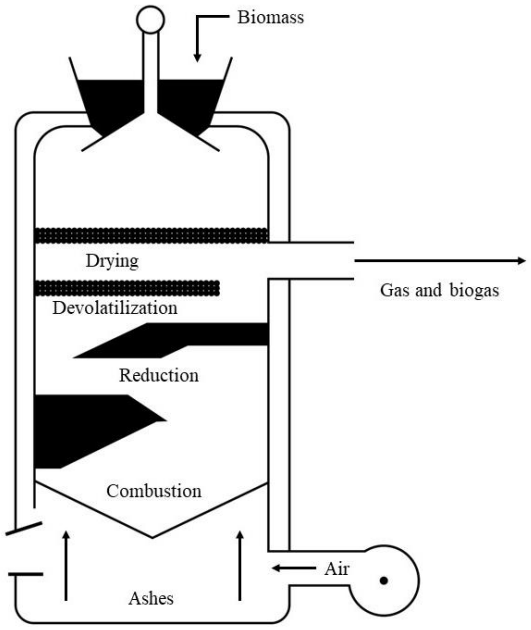


Figure 3 - Fixed bed reactor with upward flow; adapted from McKendry (2002c).

Due to the low temperature of the gas released by the reactor, the energy efficiency of the process is high, but also the released gas is rich in tar. Filtering the feed helps to produce a low particle gas (Molino, et al., 2016).

**-Fixed bed reactor with descending airflow:**

In the fixed bed reactor with descending airflow, the air direction is the same as the power supply. These gases product come out of the aerator after passing through the hot zone, allowing the partial cracking of the tars present in the gases, providing a gas with lower tar content. Figure 4 exemplifies the operation of this type of reactor. Since the product gases come out around 900-100°C, the energy efficiency of this process is low, due to the high amount of heat transported by hot gas (McKendry, 2002c).

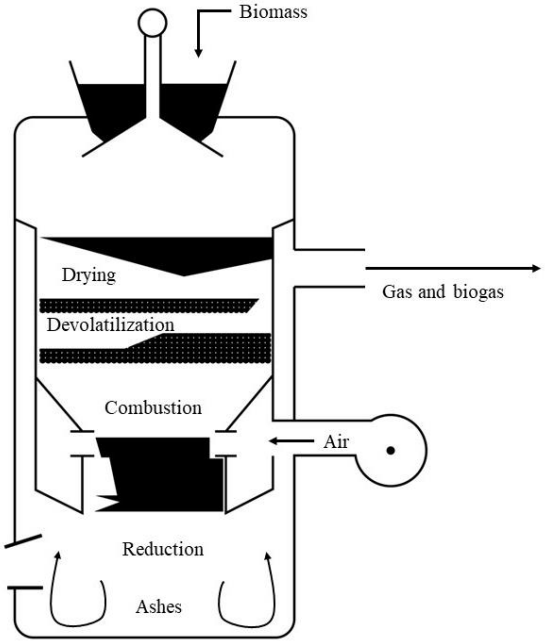


Figure 4 - Fixed bed reactor with downward flow; adapted from McKendry (2002c).

**-Fixed bed reactor with cross flow:**

In a cross-flow aerator, the feed moves down while the air is introduced laterally, and the gases are removed from the opposite side of the unit at the same level. A hot combustion/gasification zone forms around the inlet and air, with the pyrolysis and drying zones being formed further above the container. The ashes are removed from the bottom and the temperature of the gas coming out of the unit is about 800–900°C, resulting in a low overall energy efficiency for the process and a gas with high tar content (Molino et al., 2016; McKendry, 2002c).

*2.3.1.2 Fluidized bed reactor*

Fluidized bed reactors are widely used for coal gasification, their advantage under the fixed bed reactors is the uniform temperature distribution in the gasification zone. Temperature uniformity is achieved using a bed of fine grain material into which air is introduced, fluidizing the bed material, and ensuring the mixture between the bed material, hot combustion gas and fed biomass (Peterson et al., 2008; McKendry, 2002c). Currently two main types of fluidized bed reactors are used: bubbly and circulating (McKendry, 2002c).

**- Bubbling fluidized bed reactor:**

Bubbling fluidized bed aerators consist of a container with grate at the bottom through which air is introduced, the top of the grate is the moving bed of thin granulometry material in which the prepared biomass feed is introduced. The regulation of the bed temperature to 700-900°C is done by controlling the air/biomass ratio. Biomass is pyrolyzed in the hot bed to form a coal with gaseous compounds, and the high molecular weight compounds are cracked by contact with the hot bed material, giving a gaseous product with low tar content (McKendry, 2002c).

**- Circulating fluidized bed reactor:**

Circulating fluidized bed aerators are widely used in the paper industry for the gasification of shells and other materials (Mahamulkar et al., 2016). The bed material is circulated between the reaction container and a cyclone separator, where the ashes are removed and the bed material and the coal back into the reaction container. Aerators can be operated at high pressures, being the advantage for those end-use applications where gas must be compressed later, such as in a gas turbine (McKendry, 2002c).

*2.3.1.3 Catalytic bed reactor*

It is also possible in this process to introduce a catalytic bed. Using this method is introduced a catalyst to the bed, thus increasing the efficiency of the process in terms

of energy and in terms of residence time. The main products of the gasification process depend on the quality of the feed, type of aerator, feed rate, heating rate, as well as the operating conditions (temperature, pressure, oxidizing agent, etc.). (Peterson et al., 2008).

### 2.3.2 Pyrolysis

In the pyrolysis process, two types of reactors are used. For the rapid pyrolysis process, the fluid bed reactor is used and for the other pyrolysis processes the fixed bed reactor (Aravind et al., 2020) is used.

#### *2.3.2.1 Fixed-bed reactor*

In the fixed bed reactor, the biomass is previously crushed in order to reduce its granulometry. Then it is loaded in the cylindrical part and maintained inside the reactor. The reactor is kept inside a furnace that is heated externally and the temperature is controlled inside the reactor. The volatile content of the biomass is vaporized and transported out of the reactor. These gases then reach the cooling chamber and are then condensed into fuels such as bio-oil. Uncondensed vapors can be recycled and used for heating (Aravind et al., 2020, Campanella and Harold, 2012).

#### *2.3.2.2 Fluidized bed reactor*

The reactor is composed of a stable bed of particles and biomass, with or without catalyst, along with an inert gas and. A cyclone separator is used to separate the solid particles from the gas. The collected vapors are condensed, while the non-condensed ones are recycled for heating. This reactor has the advantage of reducing the catalytic cracking that occurs in pyrolysis through the rapid separation of coal and steam (Aravind et al., 2020; He et al., 2021).

## 2.4 Pyrolysis and gasification of biomass modeling processes

### 2.4.1 Simulation models

In the field of computing software interprets processes as data entry, data processing, and data return. The important thing for a computational process is to transform biomass, something of complex composition, into information that can be processed by a computer, for example by separating biomass into its elemental composition. Usually, the data inputs are mass or molar flow, temperature, pressure, and elemental composition. The most used software already has enough information in their database for the processing of this data. These studies are widely used for equipment sizing, and economic planning (Nikoo and Mahinpey, 2008).

Specifically for the pyrolysis and gasification process, modeling and simulation helps in predicting the compositions of output products, sizing equipment, planning of a plant, and still being adjusted for greater economic viability. Because it is a complex process, simulation models are divided into two types, kinetic models, and thermodynamic equilibrium (Nikoo and Mahinpey, 2008).

#### *2.4.1.1 Thermodynamic equilibrium models*

For thermodynamic equilibrium models it is assumed that the reaction is in its most stable state, i.e., less free energy. Thus, the main hypothesis is that the reactions are fast enough, and the residence time is sufficient to achieve the balance of the system. This condition is met at temperatures above 800°C. This model is not effective at lower temperatures due to the impossibility of performing these system balancing considerations (Buragohain et al., 2010).

#### *2.4.1.2 Kinetic models*

The accuracy of the data entered directly impact on the quality of the data obtained. Kinetic models employ detailed mechanisms of present chemical reactions, reaction rates, residence time and hydrodynamics. Kinetic models are very close to reality

due to these considerations, and accurately describe the behavior of the process in different parts of the system and reactor. All these factors increase the complexity of the process due to the large number of parallel reactions (Babich et al., 2011).

### 2.4.2 Simulation and modeling software

In pyrolysis and biomass gasification processes the most used simulation and modeling program is Aspen Plus (AspenTech) and Aspen HYSYS (AspenTech), however this work aims to use the UniSim Design (Honeywell) program. Aspen Plus is the most widely used program in optimization and modeling of chemical engineering processes, also in sensitivity analysis and economic evaluation. UniSim Design is a program like Aspen Plus, it is used in engineering to create dynamic and steady-state models for plant design, monitoring, troubleshooting, planning, and management. Although it is very complete, few studies use this program to perform simulation and/or modeling. This study will be fully done using UniSim Design software.

## 2.5 Operation conditions and reactions

Setting the operating parameters is very important in a simulation and in a real process. It is important to study how the parameters influence the behavior and performance of the operation, these parameters (temperature, pressure, residence time, etc.) can be changed to increase the yield of a given fuel or speed up the process. In this topic you will briefly discuss how these parameters influence the process and the main reactions at each stage of the process.

### 2.5.1 Pyrolysis

The operating conditions in this stage influence the thermodynamics and kinetics of the reaction. Babich et al. (2011) studied the pyrolysis process and found that the main products at this stage are bio-oil and charcoal.

*2.5.1.1 Main reaction*

Regarding the pyrolysis step, the generic reaction is shown in Table 3.

Table 3 - Main reaction in pyrolysis, adapted from Paiva (2020) and

| Step | Reaction |
|---|---|
| Pyrolysis | Biomass → Char + Tar + Volatiles (1) |

(1) In this step the volatiles are released, this is called devolatilization.

*2.5.1.2 Temperature effect*

The studies by Huang et al. (2016) and Ningbo et al. (2015) show that because it is an endothermic process (where heat is needed from an external source) temperature greatly influences the process. Higher temperatures and higher heating rates increase the breakdown of bonds, producing smaller molecules, directly influencing the generation of products.

*2.5.1.3 Residence time effect*

The heating rate is directly related to the time of residence, pyrolysis can be classified as slow or fast depending on your residence time, and this is defined by the heating rate, the higher the rate of heating (temperature per time) the shorter the residence time and vice versa. According to Ningbo et al. (2015), longer residence times favor a secondary conversion of primary products, producing more carbon residues, tars, and thermally more stable products. Mlonka-Mędrala et al. (2021), shows that the increase in reaction time favors the yield of more solid and gaseous products and decreases the formation of liquid products.

*2.5.1.4 Pressure effect*

According to Nguyen et al. (2016), operating at high pressure and at a high temperature peak favors the formation of pyrolysis gas, and decreases the formation of

charcoal. Low pressures reduce condensation of reactive fragments forming more carbon residue.

### 2.5.2 Gasification

As in the pyrolysis process, temperature, pressure, and residence time strongly influence the thermodynamics and kinetics of the gasification process. Thus, it is extremely important to study how these variables influence the process.

*2.5.2.1 Main reactions*

The main reactions to be used during the gasification process are shown below (see Table 4).

Table 4 - Main reactions in gasification, adapted from Maldonado (2022).

| Step | Reaction | ΔH° (kJ.mol$^{-1}$) | Reference |
|---|---|---|---|
| Combustion | $C_{10}H_8 + 12O_2 \rightarrow 10CO_2+4H_2O$ (2) | -5157 | Tool Box (2017) |
| | $C_7H_8 + 9O_2 \rightarrow 7CO_2 + 4H_2O$ (3) | -3910 | Tool Box (2017) |
| | $C_6H_6 + 7{,}5O_2 \rightarrow 6CO_2 + 3H_2O$ (4) | -3268 | Tool Box (2017) |
| | $C_{(solid)} + ½\ O_2 \rightarrow CO$ (5) | -110 | Basu (2010) |
| | $C_{(solid)} + O_2 \rightarrow CO_2$ (6) | -393 | Basu (2010) |
| | $CO + ½\ O_2 \rightarrow CO_2$ (7) | -283 | Basu (2010) |
| | $H_2 + ½\ O_2 \rightarrow H_2O$ (8) | -242 | Basu (2010) |
| | $CH_4 + 2O_2 \leftrightarrow CO_2 + 2H_2O$ (9) | -802 | Basu (2010) |
| Reduction | $C_{(solid)} + CO_2 \leftrightarrow 2CO$ (10) | 172 | Basu (2010) |
| | $C_{(solid)} + H_2O \leftrightarrow CO + H_2$ (11) | 131 | Basu (2010) |
| | $CO + H_2O \leftrightarrow CO_2 + H_2$ (12) | -42 | Basu (2010) |
| | $C_{(solid)} + 2H_2 \leftrightarrow CH_4$ (13) | -75 | Basu (2010) |
| | $CH_4 + H_2O \leftrightarrow CO + 3H_2$ (14) | 206 | Basu (2010) |

1. In this step the volatiles are released, this is called devolatilization.
2. Naphtalene oxidation: is the complete combustion of naphtalene.
3. Toluene oxidation: is the complete combustion of toluene.
4. Benzene oxidation: is the complete combustion of benzene.
5. Carbon partial oxidation: is the incomplete carbon combustion.
6. Carbon oxidation: is the carbon complete combustion.
7. Carbon monoxide oxidation: is the CO oxidation.
8. Hydrogen oxidation: is the $H_2$ oxidation.
9. Methane oxidation: is the complete methane combustion.
10. Boudoard reaction: is a process that produces CO.
11. Reforming of char: is a heterogeneous shift reaction.
12. Water gas shift reaction: is a gas-water displacement reaction.
13. Hydrogasification: is a hydrogenation reaction
14. Steam-methane reforming is the methane reforming reaction.

*2.5.2.2 Temperature effect*

Among several factors that affect process efficiency and product yield, gasification temperature should be evaluated and optimized, considering energy consumption. The increase in temperature also increases the consumption operating cost

due to heat demand. Temperature values influence the products generated, according to Janajreh et al. (2021), it is possible to relate the increase in temperature with an increase in the amount of carbon monoxide and water vapor, a decrease in the volume fraction of carbon dioxide and methane.

#### *2.5.2.3 Residence time effect*

Residence time is related to the temperature reached. The higher the temperature, the lower the residence time required because the reactions involved will be more spontaneous and vice versa. The increase in residence time allows to reach a state closer to chemical equilibrium as well as a more efficient decomposition of the formed tar (Chen et al., 2020).

#### *2.5.2.4 Pressure effect*

Chen et al. (2020), studied the effect of pressure on the biomass gasification reaction and found that higher pressures in the reactor increase. This indicates that the higher pressure promotes the reverse reform reaction of $CO_2$. High pressure also has a positive effect on supercritical water gasification, for example, high pressure leads to an increase in the density of supercritical water and ionic products. Thus, hydrolysis reactions and extraction of the volatile component of coal reactions and pyrolysis are promoted under high pressure.

# *Part 3 - Methodology*

The chosen methodology is divided in two parts: the first focusing on the modeling of biomass pyrolysis using a non-isothermal kinetic model to be performed in Python language, the non-isothermal model was chosen to vary the temperature with the time, the second will be the implementation of the pyrolysis model developed in the software and later the simulation is finalized implementing the other necessary gasification steps.

Focusing on reducing data analysis, two types of biomasses will be analyzed: olive pit and wood residue (see Table 5).

Table 5 - Analyzed biomass composition

| Type of biomass | VM (%) | FC (%) | W (%) | Ashes (%) | C (%) | O (%) | H (%) | N (%) | S (%) | Reference |
|---|---|---|---|---|---|---|---|---|---|---|
| Wood residue | 57.4 | 12.2 | 26.4 | 4.0 | 51.4 | 41.9 | 6.1 | 0.5 | 0.08 | Miles *et al*. (1995) |
| Olive pit | 72.3 | 18.7 | 6.1 | 2.9 | 52.8 | 39.4 | 6.6 | 1.1 | 0.07 | Vamvuka and Zografos. (2004) |

## 3.1 Fast pyrolysis model

In the pyrolysis stage, the objective was to decompose biomass, a complex solid, into less complex gases, solids, and liquids, which can be added to SBM in the software.

### 3.1.2 Kinetic non-isothermal model

The model chosen was the non-isothermal kinetic model proposed by Babu and Charausia (2003) which is based on the Koufopanos et al. (1991) model, along with the model of Srivastava et al. (1996). The model proposes the following two-step mechanism scheme to describe the kinetics of biomass pyrolysis:

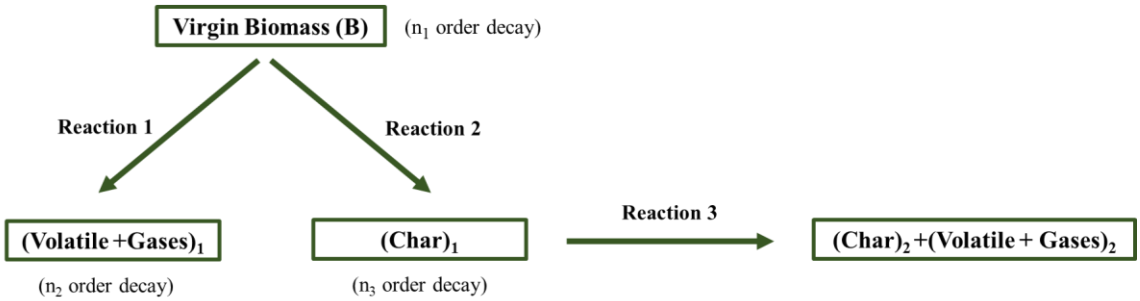


Figure 5 - Two step mechanism biomass pyrolysis, adapted from Babu and Chaurasia (2003).

This model assumes that biomass decomposes into volatiles, gases, and coal (solid part). Subsequently the volatiles and gases react with coal producing other types of volatiles, gases, and coal of different compositions. Below are the kinetic equations of the selected mechanism:

$$\frac{dC_b}{dt} = k_1 C_b^{n1} - k_2 C_b^{n1} \quad (1)$$

$$\frac{dC_{G1}}{dt} = k_1 C_b^{n1} - k_3 C_{G1}^{n2} C_{C1}^{n3} \quad (2)$$

$$\frac{dC_{C1}}{dt} = k_1 C_b^{n1} - k_3 C_{G1}^{n2} C_{C1}^{n3} \quad (3)$$

$$\frac{dC_{G2}}{dt} = k_3 C_{G1}^{n2} C_{C1}^{n3} \quad (4)$$

$$\frac{dC_{C2}}{dt} = k_3 C_{G1}^{n2} C_{C1}^{n3} \quad (5)$$

Where constants $k_i$ are function of temperature:

$$k_1 = A_1 \exp\left[\left(\frac{D_1}{T} - \frac{L_1}{T^2}\right)\right] \quad (6)$$

$$k_2 = A_2 \exp\left[\left(\frac{D_2}{T} - \frac{L_2}{T^2}\right)\right] \quad (7)$$

$$k_3 = A_3 \exp\left[\left(\frac{-E_3}{RT}\right)\right] \quad (8)$$

And the constants according to the model are:

$A_1 = 9.973 \times 10^{-5}\ (s^{-1})$ $A_2 = 1.068 \times 10^{-3}\ (s^{-1})$ $A_3 = 5.7 \times 10^{-5}\ (s^{-1})$

$D_1 = 17254.4\ (K)$ $D_2 = 10224.4\ (K)$

$L_1 = -9061227\ (K^2)$ $L_2 = -3123081\ (K^2)$

$E_3 = 81\ (kJ/mol)$ $R = 8.314\ J/K.mol$

Another important equation used is the temperature variation as a function of time, this equation proposed by Srivastava et al. (1996) is presented below:

$$T = (HR)t + T_0 \quad (9)$$

Then, according to the model, four variables are used: time, temperature, heating rate and initial biomass concentration.

### 3.1.3 Pyrolysis solution proposal

The first major difficulty would be to solve the ODE's system simultaneously, for this was used numerical integration, the Fourth Order Runge-Kutta method. Using Python, a program was developed that has as initial inputs: elemental composition (carbon and sulfur in %), mass flow (in kg/h), initial temperature (in K), heating rate (constant in K/s) and final time (in s).

With the initial data and model equations 1-9 it is possible to obtain the first results: $C_b$, $C_{C1}$, $C_{G1}$, $C_{C2}$ and $C_{G2}$. This is not yet the expected result of this stage, because although it is already possible to estimate the concentrations of gases, volatiles, and coal, it is still unknown specifically the composition of these elements. In this way, the following considerations were made:

I. The volatile concentration is equal to $C_{G1} + C_{G2}$.
II. The concentration of coal is equal to $C_{C1} + C_{C2}$.

III.The biomass that did not react, and ash is equal to 1-$C_b$.

*3.1.3.1 Volatiles composition*

Due to the model being proposed for high temperatures (usually starting at 700 K), it was then assumed that the concentration of volatiles is:

$$yVolatiles = yGases + yTar$$

$$yGases = yCO + yCO_2 + yCH_4 + yH_2$$

$$yTar = yBenzene + yToluene + yNaphtalene$$

To perform the separation and obtain the fractions of gases and tar, a polynomial regression was performed with data from the literature and an equation was obtained as a function of temperature (Neves et al., 2011):

$$yGases = \frac{(0.0001\,T^2 - \ 0.0817\,T + \ 50.502)}{200} \quad (10)$$

$$yTar = 1 - yGases \quad (11)$$

In the tar fraction, 60, 20 and 20% were considered respectively for benzene, toluene and naphtalene (Ahmad et al. 2016). The following equations were obtained:

$$yBenzene = 0.6\,yTar \quad (12)$$

$$yToluene = 0.2\,yTar \quad (13)$$

$$yNaphtalene = 0.2\,yTar \quad (14)$$

For the part of the gas fraction calculation, it was considered the methodology proposed by Trninić et al. (2020) based on second-order equations for the separation of the main gaseous products of pyrolysis, this model is less accurate at temperatures higher than 1000 K presenting negative mass fractions for carbon monoxide and carbon dioxide. Then it was considered that when the fraction of these gases is less than zero it is equal to zero. Then the following equations are proposed from the model:

$$yCO = yGases * (-2.65\,T^2 * 10^{-4} - 0.27 * T - 32.71)/100 \quad (15)$$

$$yCO_2 = yGases * (-2.85\,T^2 * 10^{-5} - 0.029 * T + 70.89)/100 \quad (16)$$

$$yCH_4 = yGases * (6.69\,T^2 * 10^{-5} - 0.037 * T + 4.28)/100 \quad (17)$$

$$yH_2 = yGases * (7\,T^2 * 10^{-5} - 0.0371 * T + 5.11)/100 \quad (18)$$

*3.1.3.2 Charcoal composition*

Solid products are the other part described by the model, this part encompasses solid carbon, and ashes of complex composition. In the solid product part, it was considered that:

i. The solid fraction is composed of ash and solid carbon.
ii. The ash fraction is carbon-free.
iii. The residue is composed by ash.
iv. The initial sulfur and water mass is equal to the finish.

To discover the carbon composition of the solid part a mass balance was carried out from the initial carbon and the carbon of the products. Performing stochiometric calculations based on the amount of initial carbon, the products containing carbon formed and the fraction of solids from the initial mass it was possible to perform the mass balance according to the balance:

$$\text{Carbon}_{(mol)} = \text{yChar} * (\text{Carbon}_{initial(mol)} - \text{CO}_{(mol)} - \text{CO}_{2(mol)} - \text{CH}_{4(mol)} - 6\,\text{Benzene}_{(mol)} - 7\,\text{Toluene}_{(mol)} - 10\,\text{Naphthalene}_{(mol)})$$

The mass balance of sulfur and water is easier, as it remains constant all the time. Being represented by:

$$\text{Sulfur}_{(mol)} = \text{Sulfur}_{initial(mol)}$$

$$\text{Water}_{(mol)} = \text{Water}_{initial(mol)}$$

To complete the balance, it is necessary to add a last various, responsible for correcting the balance. This represents the residual biomass and the ash of the coal part:

$$yResidual = 1 - yS_{(solid)} - yWater - yCO - yCH_4 - yH_2 - yBenzene - yToluene - yNaphtalene - yCarbon_{(solid)}$$

## 3.2 Biomass pyrolysis and gasification on Unisim Design

After realized the calculations of biomass pyrolysis, the complete simulation in downdraft was performed in the Unisim Design software (see figure 6):

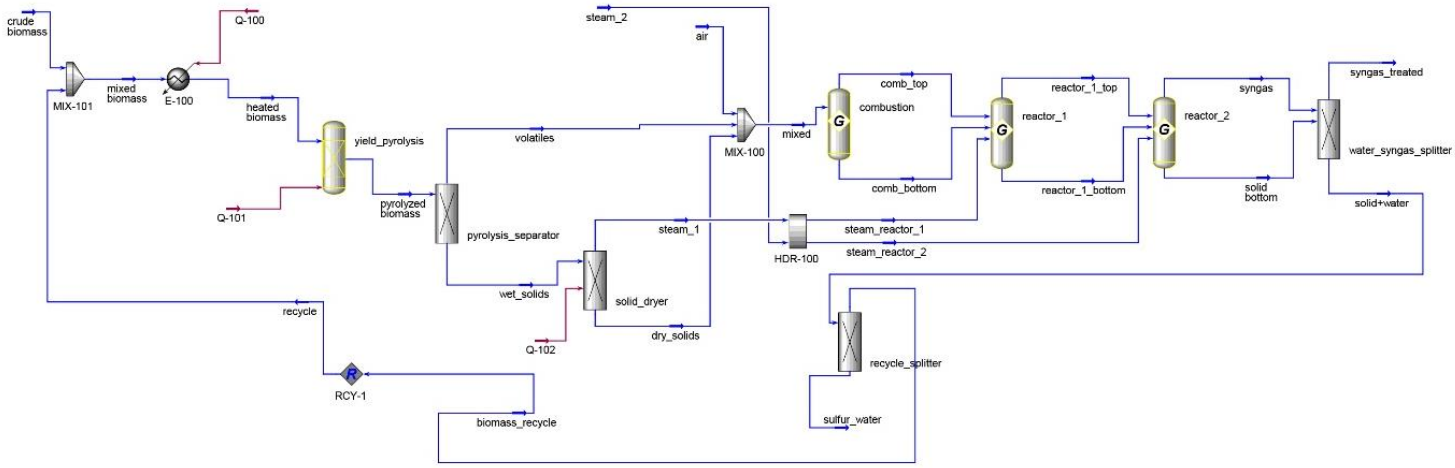


Figure 6 - Pyrolysis and gasification of biomass PFD.

### 3.2.1 Simulation step 1 - Pyrolysis

The first step is to heat the biomass up to 700 K to perform the fast pyrolysis process in a fluidized bed reactor. As the model described above does not have a yield of 100%, a part of the biomass will be loaded during the process and later a cycle current is added. The raw biomass is mixed with the unreacted biomass of the cycle current in the

block "MIX-101", after this the biomass is sent to a heater "E-100" and proceeds to the Yield reactor where the pyrolysis process will be performed with the respective conversions calculated following the pyrolysis model presented. After that a "pyrolysis_separator" separator separates the pyrolyzed biomass into two volatiles and "wet_solids".

### 3.2.2 Simulation step 2 – Biomass drying

The flow of wet solids is sent to a "solid_dryer" dryer powered by a "Q-102" power current that aims to remove water from the solids. The steam removed "steam_1" proceeds to a header that mixes this steam with another external current "steam_2" which will later distribute the steam to reactors 1 and 2. Dry solids proceed to a "MIX-100" mixer together with an external air stream and volatiles from the pyrolysis process.

### 3.2.3 Simulation step 3 – Combustion

The "mixed" line is sent to an adiabatic Gibbs reactor where the "Combustion" reaction set of table 4 will be performed. The products of this "comb_top" and "comb_bottom" process will proceed to reactor 1.

### 3.2.4 Simulation step 4 – Reduction

The "reactor_1" block is powered by a steam current "steam_reactor_1" and the products of the combustion reactor, this first reactor is responsible for heterogeneous reduction. The products of reactor 1 proceed to reactor 2, which is also powered by a steam current "steam_reactor_2", in this reactor are performed the steps of homogeneous reduction. The products of this reactor are the chains of syngas and solids that will be treated later.

### 3.2.5 Simulation step 5 – Syngas treating

The last "water_syngas_splitter" block aims to remove solids and water from the syngas, the products are: "syngas_treated" and "solid+water". The upper current is composed of treated syngas, the current composed of solids and water proceeds to a "recycle_splitter" separator that separates water and sulfur from the unreacted biomass. Unreacted biomass is recycled and remixed to the initial mixer.

## 3.3 Standard simulation and considerations

In this topic it will be covered the defined considerations about the simulation. The following table presents the data related to operating conditions for the material currents in each of the simulation steps, on a biomass/steam and biomass/air equivalence ratio of 1 (mole basis), the chosen biomass is due the different carbon and moisture content, with olive pit with a higher carbon content and wood residue more water in its composition.

Table 6 – Olive pit material streams standard data

| *Olive pit* | | | | |
|---|---|---|---|---|
| *Step 1* | | | | |
| **Name** | **crude biomass** | **volatiles** | **wet_solids** | |
| Vapour Fraction | 0.00 | 1.00 | 0.33 | |
| Temperature [°C] | 24.85 | 1126.85 | 1126.90 | |
| Pressure [kPa] | 101.30 | 101.30 | 101.30 | |
| Molar Flow [kgmol/h] | 10.00 | 39.49 | 2.16 | |
| Mass Flow [kg/h] | 202.25 | 175.78 | 32.94 | |
| Liquid Vol. Flow [$m^3$/h] | 0.15 | 1.27 | 0.03 | |
| Heat Flow [kJ/h] | $-1.14\times10^6$ | $1.28\times10^6$ | $-1.37\times10^5$ | |
| *Step 2* | | | | |
| **Name** | **dry_solids** | | **Air** | |
| Vapour Fraction | 0.00 | | 1.00 | |
| Temperature [°C] | 1126.85 | | 175.00 | |
| Pressure [kPa] | 101.30 | | 101.30 | |
| Molar Flow [kgmol/h] | 1.46 | | 10.00 | |
| Mass Flow [kg/h] | 20.21 | | 291.69 | |
| Liquid Vol. Flow [$m^3$/h] | 0.01 | | 0.33 | |
| Heat Flow [kJ/h] | $2.93\times10^3$ | | $4.44\times10^4$ | |
| *Step 3* | | | | |
| **Name** | **mixed** | **comb_ top** | **comb_bottom** | |
| Vapour Fraction | 0.97 | 1.00 | 0.00 | |
| Temperature [°C] | 966.65 | 1143.93 | 1143.93 | |
| Pressure [kPa] | 101.30 | 101.30 | 101.30 | |
| Molar Flow [kgmol/h] | 50.94 | 56.37 | 0.32 | |
| Mass Flow [kg/h] | 487.68 | 481.06 | 6.62 | |
| Liquid Vol. Flow [$m^3$/h] | 1.61 | 1.74 | 0.00 | |
| Heat Flow [kJ/h] | $1.33\times10^6$ | $1.3\times10^6$ | $-1.93\times10^4$ | |
| *Step 4* | | | | |
| **Name** | **steam_1** | **steam_2** | **syngas** | **solid bottom** |
| Vapour Fraction | 1.00 | 1.00 | 1.00 | 0.00 |
| Temperature [°C] | 99.95 | 149.85 | 924.42 | 924.42 |
| Pressure [kPa] | 101.30 | 474.14 | 101.30 | 101.30 |
| Molar Flow [kgmol/h] | 0.71 | 10.00 | 68.20 | 0.32 |
| Mass Flow [kg/h] | 12.73 | 180.15 | 673.95 | 6.62 |
| Liquid Vol. Flow [$m^3$/h] | 0.01 | 0.18 | 1.99 | 0.00 |
| Heat Flow [kJ/h] | $-1.69\times10^5$ | $-2.4\times10^6$ | $-1\times10^6$ | $-2.33\times10^4$ |
| *Step 5* | | | | |
| **Name** | **syngas_ treated** | **solid+ water** | **biomass_recycle** | |
| Temperature [°C] | 1264.73 | 99.95 | 99.85 | |
| Molar Flow [kgmol/h] | 59.04 | 9.49 | 0.32 | |
| Liquid Vol. Flow [$m^3$/h] | 1.82 | 0.17 | 0.00 | |
| Heat Flow [kJ/h] | $1.38\times10^6$ | $-2.6\times10^6$ | $-3.57\times10^4$ | |

Table 7 - Wood residue material streams standard data

| *Wood residue* | | | | |
|---|---|---|---|---|
| *Step 1* | | | | |
| **Name** | **crude biomass** | **volatiles** | **wet_solids** | |
| Vapour Fraction | 0.00 | 1.00 | 0.38 | |
| Temperature [°C] | 24.85 | 1126.85 | 1126.92 | |
| Pressure [kPa] | 101.30 | 101.30 | 101.30 | |
| Molar Flow [kgmol/h] | 10.00 | 40.71 | 1.90 | |
| Mass Flow [kg/h] | 208.54 | 181.25 | 27.29 | |
| Liquid Vol. Flow [$m^3$/h] | 0.15 | 1.31 | 0.02 | |
| Heat Flow [kJ/h] | $-1.56\times10^6$ | $1.32\times10^6$ | $-1.19\times10^5$ | |
| *Step 2* | | | | |
| **Name** | **dry_solids** | | **Air** | |
| Vapour Fraction | 0.00 | | 1.00 | |
| Temperature [°C] | 1126.85 | | 24.85 | |
| Pressure [kPa] | 101.30 | | 101.30 | |
| Molar Flow [kgmol/h] | 1.17 | | 10.00 | |
| Mass Flow [kg/h] | 14.16 | | 291.69 | |
| Liquid Vol. Flow [$m^3$/h] | 0.01 | | 0.33 | |
| Heat Flow [kJ/h] | $2.56\times10^4$ | | $-1.27\times10^2$ | |
| *Step 3* | | | | |
| **Name** | **Mixed** | **comb_ top** | **comb_bottom** | |
| Vapour Fraction | 0.98 | 1.00 | 0.00 | |
| Temperature [°C] | 946.54 | 946.54 | 946.54 | |
| Pressure [kPa] | 101.30 | 101.30 | 101.30 | |
| Molar Flow [kgmol/h] | 51.89 | 50.71 | 1.17 | |
| Mass Flow [kg/h] | 487.11 | 472.95 | 14.16 | |
| Liquid Vol. Flow [$m^3$/h] | 1.65 | 1.64 | 0.01 | |
| Heat Flow [kJ/h] | $1.34\times10^6$ | $1.32\times10^6$ | $2.08\times10^4$ | |
| *Step 4* | | | | |
| **Name** | **steam_1** | **steam_2** | **syngas** | **solid bottom** |
| Vapour Fraction | 1.00 | 1.00 | 1.00 | 0.00 |
| Temperature [°C] | 99.95 | 149.85 | 849.12 | 849.12 |
| Pressure [kPa] | 101.30 | 474.14 | 101.30 | 101.30 |
| Molar Flow [kgmol/h] | 0.73 | 10.00 | 60.28 | 0.00 |
| Mass Flow [kg/h] | 13.13 | 180.15 | 680.23 | 0.15 |
| Liquid Vol. Flow [$m^3$/h] | 0.01 | 0.18 | 1.83 | 0.00 |
| Heat Flow [kJ/h] | $-1.74\times10^5$ | $-2.4\times10^6$ | $-1.21\times10^6$ | $1.73\times10^3$ |
| *Step 5* | | | | |
| **Name** | **syngas_ treated** | **solid+ water** | **biomass_recycle** | |
| Temperature [°C] | 1228.40 | 99.95 | 99.85 | |
| Molar Flow [kgmol/h] | 49.55 | 10.73 | 0 | |
| Liquid Vol. Flow [$m^3$/h] | 1.63 | 0.19 | 0 | |
| Heat Flow [kJ/h] | $1.80\times10^6$ | $-3.01\times10^6$ | 0 | |

# *Part 4 - Results and discussion*

## 4.1 Pyrolysis

### 4.1.1 Pyrolysis kinetic non-isothermal model

The first kinetic model proposed by Babu and Charausia (2003) was calculated for two different types of biomasses and different compositions. The data obtained for the first stage are represented through Figures 7 and 8:

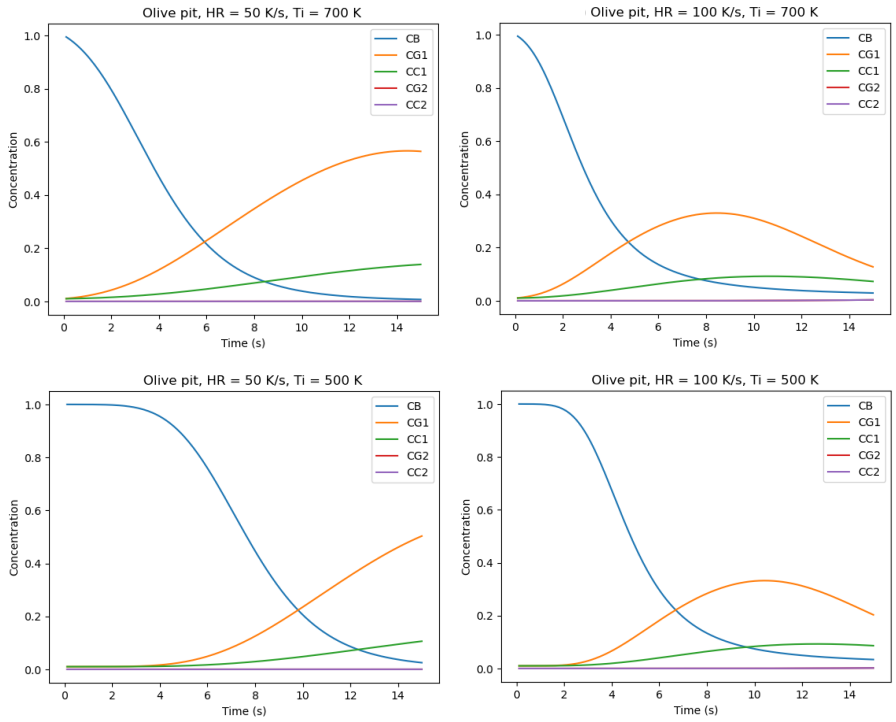


Figure 7 - Olive pit at different temperatures and heating rates, kinetic model.

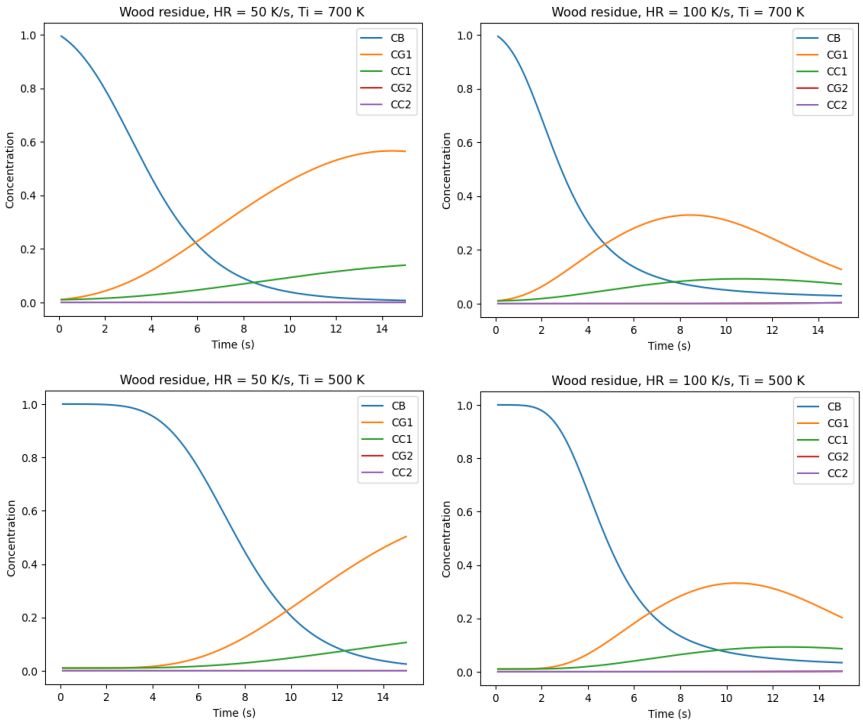


Figure 8 - Wood residue at different temperatures and heating rates, kinetic model.

For heating rates equal to 10 and 15 K/s (see Figure 9) pyrolysis was shown to be slower, leading to a more time-consuming process with lower yield, so a time of 25 seconds was stipulated to perform the pyrolysis process. For times longer than this it was observed that the model did not behave very well, demonstrating that the use of higher heating rates is preferable.

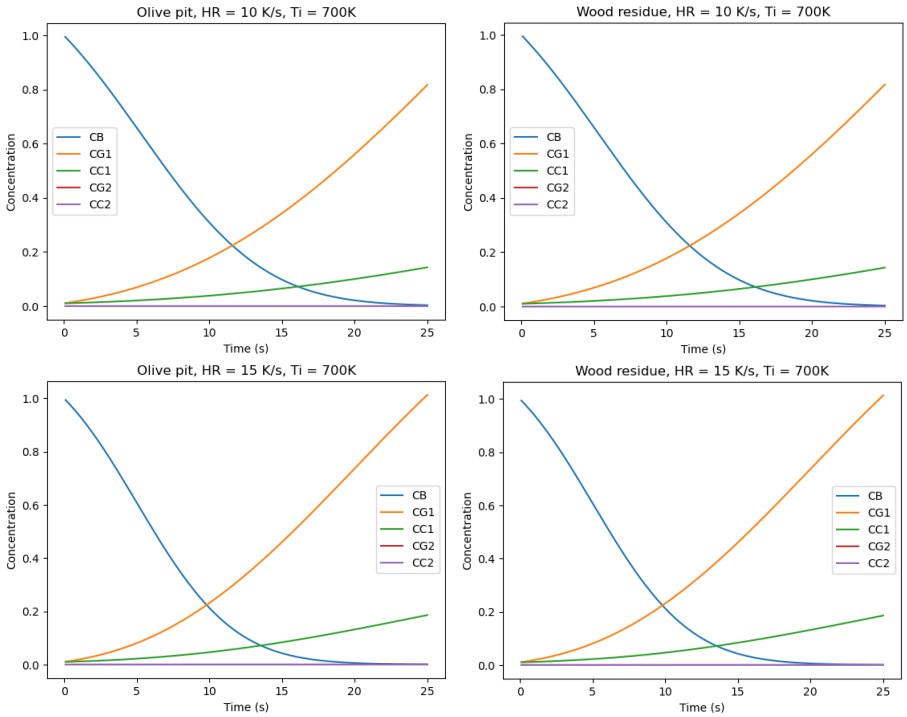


Figure 9 - Wood residue and olive pit at different temperatures and heating rates.

From the data of the kinetic model, it was possible to trace the second results by adding the curves of volatiles, solids, and unreacted biomass to visualize more accurately the behavior of the kinetic model (see Figures 10 and 11).

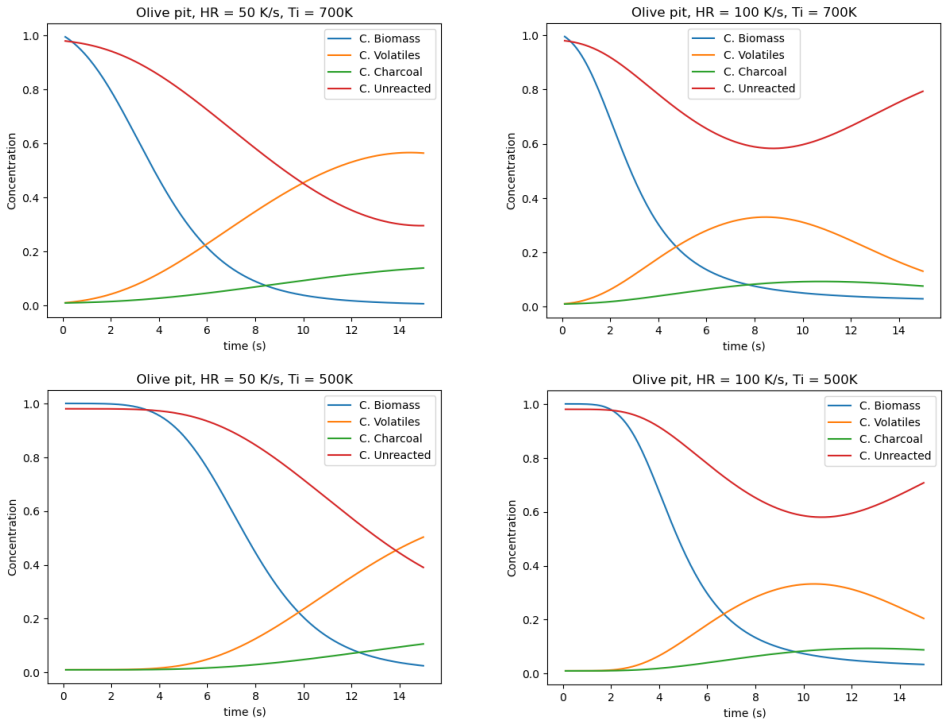


Figure 10 - Olive pit general composition at different temperatures and heating rates.

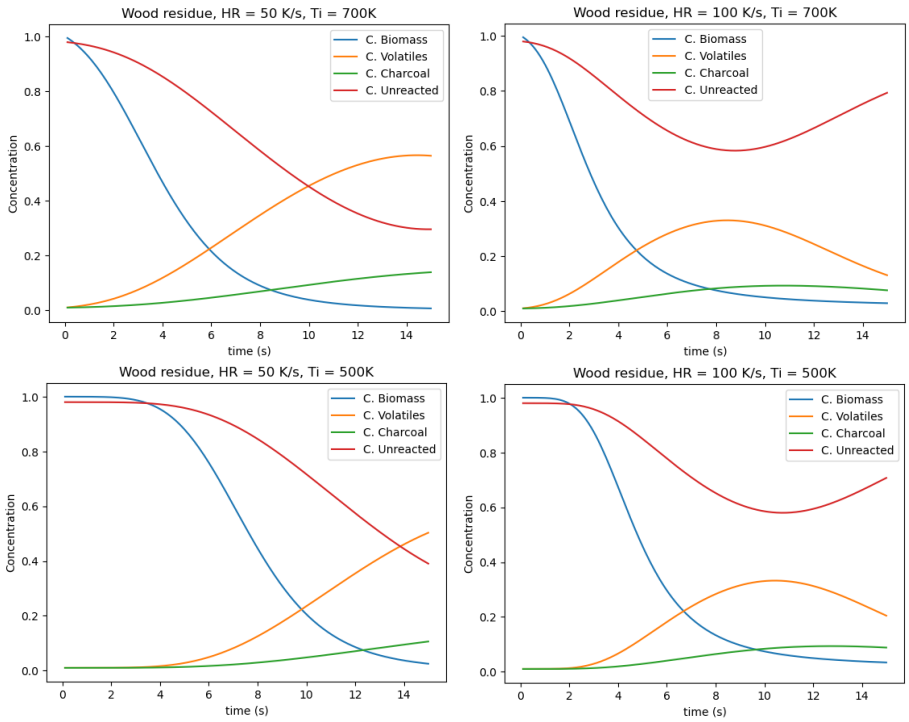


Figure 11 - Wood residue general composition at different temperatures and heating rates.

The trends observed in the figures is qualitatively the same as that of Srivastava et al. (1996) and Babu and Chaurasia (2003), but with slightly different final scores in terms of magnitude. This may be due to the use of different methods solutions and assumptions made, Srivastava et al. (1996) using the fourth order Runge-Kutta predictive-correction method simulates the model, assuming a maximum time of 20 seconds for the simulation, which is not simulated on a stopped basis in this study the time standard is 15 seconds.

Analyzing the curves, it is possible to verify that the model from high temperatures (above 1500 K) becomes less faithful, and the mass balance no longer makes sense because it leads to negative mass fractions, the optimized heating rate is around 50 K per second and the initial temperature has better results starting close to 700 K, this set shows a good relation of energy demand and yield. Results obtained from the analysis of the curves are like those obtained by Babu and Charausia (2003), in which they obtained optimized values for the model, with heating rate equal to 51 K per second and initial temperature of 773 K, and pyrolysis time equal to 9.53 seconds. Thus, in the present study

these conditions for heating rate, initial temperature and pyrolysis time will be used as a reference to continue with the gasification process.

### 4.1.2 Pyrolysis mixed model

After separation of phases by the kinetic model, the thermodynamic model was implemented to distinguish the products and predict the compositions of the phases. The results obtained from this model are represented at different temperatures and heating rates below in Figures 12 and 13.

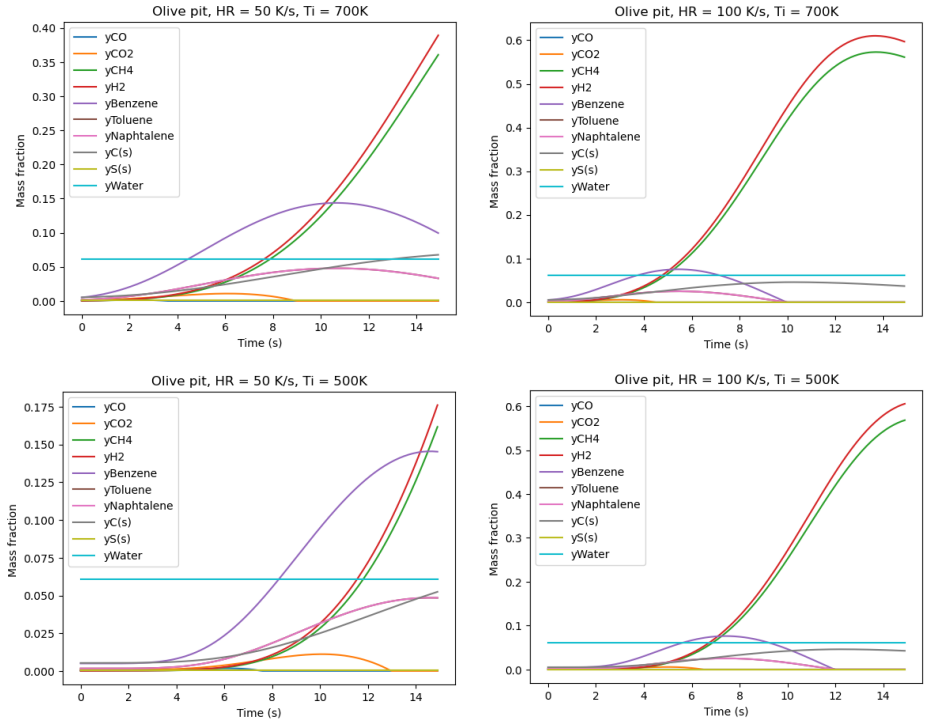


Figure 12 - Volatiles and char composition from olive pit.

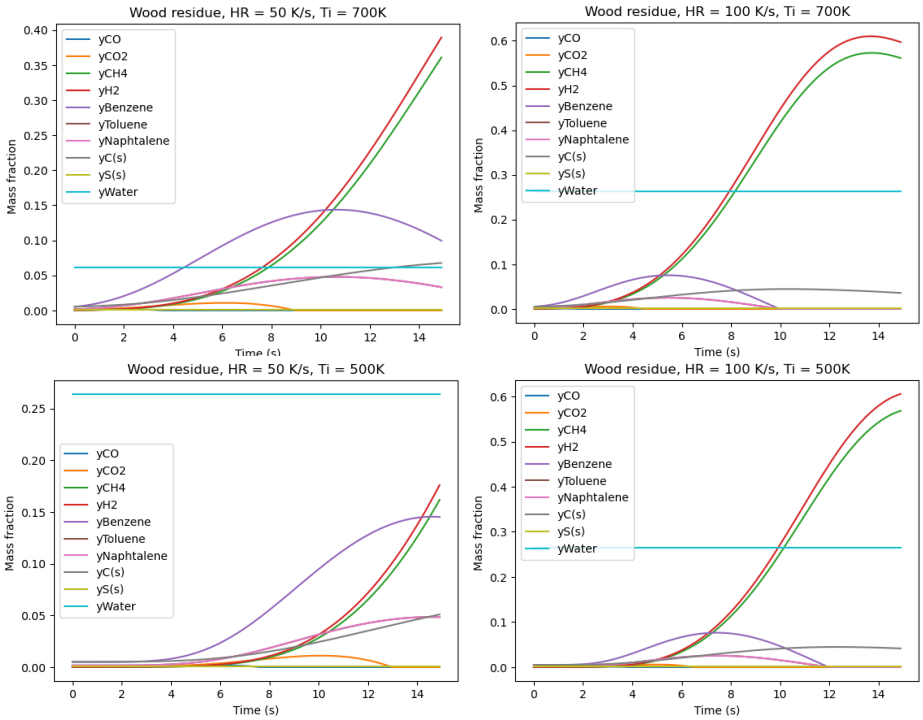


Figure 13 - Volatiles and char composition from wood residue.

According to the model high temperatures favor the formation of gaseous products ($CH_4$ and $H_2$), as previously mentioned at very high temperatures the model does not behave well, the main reason for this is because de thermodynamic second order model and the second order regression by experimental data to predict the composition of volatiles and solids used, this can be observed because in the curves of heating rate equal to 100 K/s there is a lot of formation of methane and hydrogen gas, while the formation of other products is very low. At very high temperatures the model generates negative fractions of some compounds, which is impossible, so, the process of pyrolysis will be stopped before it. Then, using the initial temperature of 700 K and heating rate equal to 50 K/s. the composition data obtained are presented in Table 8 and 9.

Table 8 - Volatiles from olive pit composition.

| Time (s) | Temp (K) | yCO | $yCO_2$ | $yCH_4$ | $yH_2$ | yBenz | yTol | yNaph |
|---|---|---|---|---|---|---|---|---|
| 0 | 700 | 0.0574 | 0.0796 | 0.0242 | 0.0292 | 0.4857 | 0.1619 | 0.1619 |
| 1 | 750 | 0.0488 | 0.0780 | 0.0334 | 0.0393 | 0.4803 | 0.1601 | 0.1601 |
| 5 | 950 | 0.0000 | 0.0593 | 0.0994 | 0.1113 | 0.4380 | 0.1460 | 0.1460 |
| 8 | 1100 | 0.0000 | 0.0185 | 0.1832 | 0.2016 | 0.3580 | 0.1193 | 0.1193 |
| 10 | 1200 | 0.0000 | 0.0000 | 0.2499 | 0.2729 | 0.2863 | 0.0954 | 0.0954 |
| 12 | 1300 | 0.0000 | 0.0000 | 0.3134 | 0.3402 | 0.2078 | 0.0693 | 0.0693 |
| 13 | 1350 | 0.0000 | 0.0000 | 0.3432 | 0.3718 | 0.1710 | 0.0570 | 0.0570 |
| 14 | 1400 | 0.0000 | 0.0000 | 0.3710 | 0.4010 | 0.1368 | 0.0456 | 0.0456 |
| 15 | 1445 | 0.0000 | 0.0000 | 0.3939 | 0.4251 | 0.1086 | 0.0362 | 0.0362 |

Table 9 - Volatiles from wood residue composition.

| Time (s) | Temp (K) | yCO | $yCO_2$ | $yCH_4$ | $yH_2$ | yBenz | yTol | yNaph |
|---|---|---|---|---|---|---|---|---|
| 0 | 700 | 0.0574 | 0.0796 | 0.0242 | 0.0292 | 0.4857 | 0.1619 | 0.1619 |
| 1 | 750 | 0.0488 | 0.0780 | 0.0334 | 0.0393 | 0.4803 | 0.1601 | 0.1601 |
| 5 | 950 | 0.0000 | 0.0593 | 0.0994 | 0.1113 | 0.4380 | 0.1460 | 0.1460 |
| 8 | 1100 | 0.0000 | 0.0185 | 0.1832 | 0.2016 | 0.3580 | 0.1193 | 0.1193 |
| 10 | 1200 | 0.0000 | 0.0000 | 0.2499 | 0.2729 | 0.2863 | 0.0954 | 0.0954 |
| 12 | 1300 | 0.0000 | 0.0000 | 0.3134 | 0.3402 | 0.2078 | 0.0693 | 0.0693 |
| 13 | 1350 | 0.0000 | 0.0000 | 0.3432 | 0.3718 | 0.1710 | 0.0570 | 0.0570 |
| 14 | 1400 | 0.0000 | 0.0000 | 0.3710 | 0.4010 | 0.1368 | 0.0456 | 0.0456 |
| 15 | 1445 | 0.0000 | 0.0000 | 0.3939 | 0.4251 | 0.1086 | 0.0362 | 0.0362 |

And the solid products compositions are presented in Tables 10 and 11.

Table 10 - Solids composition from olive pit.

| Time (s) | Temp (K) | $yC_{(s)}$ | yWater | $yS_{(s)}$ | yUnreacted |
|---|---|---|---|---|---|
| 0 | 700 | 0.0054 | 0.0616 | 0.0007 | 0.9322 |
| 1 | 750 | 0.0066 | 0.0624 | 0.0007 | 0.9303 |
| 5 | 950 | 0.0231 | 0.0731 | 0.0008 | 0.9030 |
| 8 | 1100 | 0.0548 | 0.0940 | 0.0011 | 0.8501 |
| 10 | 1200 | 0.0936 | 0.1216 | 0.0014 | 0.7834 |
| 12 | 1300 | 0.1723 | 0.1837 | 0.0021 | 0.6419 |
| 13 | 1350 | 0.2517 | 0.2498 | 0.0029 | 0.4956 |
| 14 | 1400 | 0.4124 | 0.3865 | 0.0044 | 0.1966 |
| 15 | 1445 | 0.5231 | 0.4715 | 0.0054 | 0.0000 |

Table 11 - Solids composition from wood residue.

| Time (s) | Temp (K) | $yC_{(s)}$ | yWater | $yS_{(s)}$ | yUnreacted |
|---|---|---|---|---|---|
| 0 | 700 | 0.0053 | 0.2668 | 0.0008 | 0.7271 |
| 1 | 750 | 0.0064 | 0.2700 | 0.0008 | 0.7227 |
| 5 | 950 | 0.0225 | 0.3164 | 0.0010 | 0.6602 |
| 8 | 1100 | 0.0533 | 0.4069 | 0.0012 | 0.5386 |
| 10 | 1200 | 0.0910 | 0.5261 | 0.0016 | 0.3814 |
| 12 | 1300 | 0.1673 | 0.7952 | 0.0024 | 0.0350 |
| 13 | 1350 | 0.1840 | 0.8135 | 0.0025 | 0.0000 |
| 14 | 1400 | 0.1927 | 0.8049 | 0.0024 | 0.0000 |
| 15 | 1445 | 0.1988 | 0.7987 | 0.0024 | 0.0000 |

### 4.1.3 Pyrolysis heat flow

Next, the study of the energy needed to convert the products was carried out, starting from a temperature in the initial reactor of 700 K, the results obtained are as follows on the x-axis this represented the temperature value of the pyrolithic reactor and on the y-axis the energy value required to reach such temperature. The study shows that the heating rate is constant: As expected, the required energy value is directly connected with the reactor temperature, the increase in temperature provides a higher energy demand.

### 4.1.4 Pyrolysis final data

To proceed with the simulation, the data that presented the most reasonable result to proceed with the simulation were selected, and the data were selected: Temperature and solids/volatiles compositions. This data is presented in Table 12.

Table 12 - Pyrolysis final data, mass fractions.

| **Biomass** | **T(K)** | **y$CH_4$** | **y$H_2$** | **yBenz** | **yTol** | **yNaph** | **yC(s)** | **yWater** | **yS(s)** | **yUnreacted** |
|---|---|---|---|---|---|---|---|---|---|---|
| Olive pit | 1400 | 0.312 | 0.337 | 0.1152 | 0.0384 | 0.0384 | 0.0651 | 0.0610 | 0.0007 | 0.0310 |
| Wood residue | 1300 | 0.209 | 0.227 | 0.1388 | 0.0463 | 0.0463 | 0.0556 | 0.2640 | 0.0008 | 0.0116 |

At this temperature there is no formation of carbon dioxide and monoxide according to the model, so these data were not presented in the table.

## 4.2 Syngas composition

After the simulation is finished, the ratio of air and steam intake with a fixed biomass mass (10 kgmol/h) was studied, the air and steam flows were varied from 5 to 20 kgmol/h, respectively, an equivalence of 0.5 to 2 mols of steam/air by biomass moles. The composition of the main components of the synthesis gas was studied: Hydrogen, carbon monoxide, carbon dioxide, oxygen, and methane, but in some cases the synthesis gas also presented a certain composition of nitrogen and naphthalene. In the figures, the vertical axis represents the variation of the molar air flow, and the curves have a constant flow "state var" of steam.

### 4.2.1 Carbon monoxide

Figures 14 to 17 represent the study of the influence of the variation of air and vapor inlet flows on the composition of carbon monoxide in the synthesis gas.

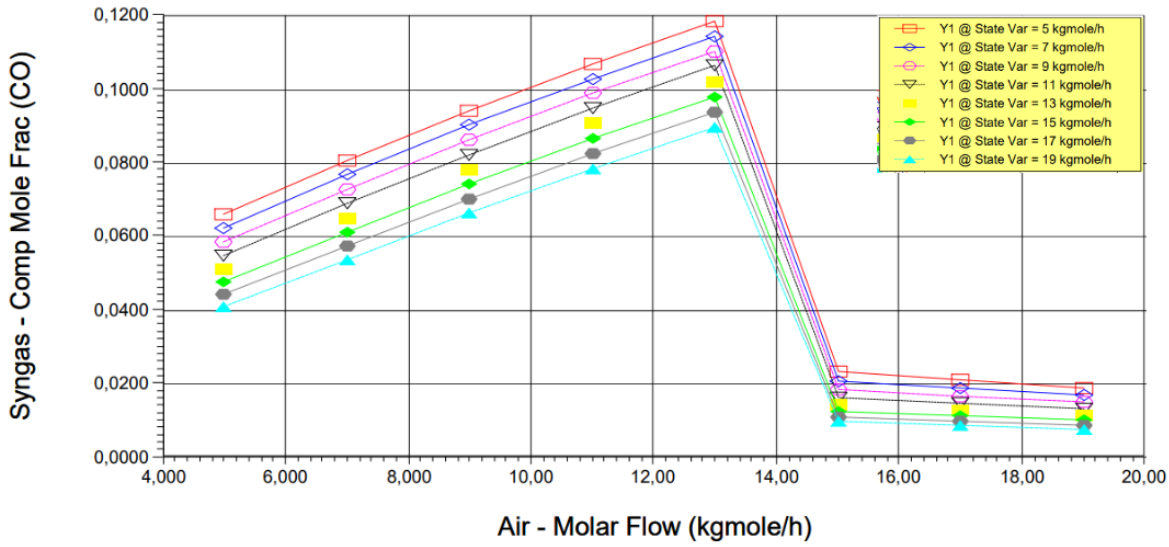


Figure 14 - Olive pit carbon monoxide composition (mole).

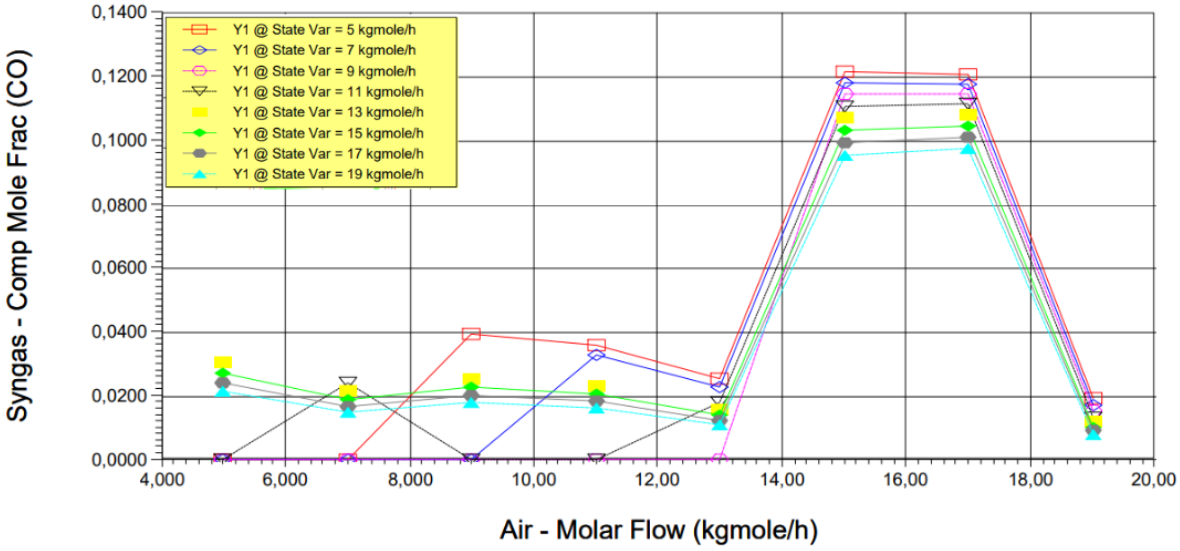


Figure 15 - Wood residue carbon monoxide composition (mole).

And in mass fractions:

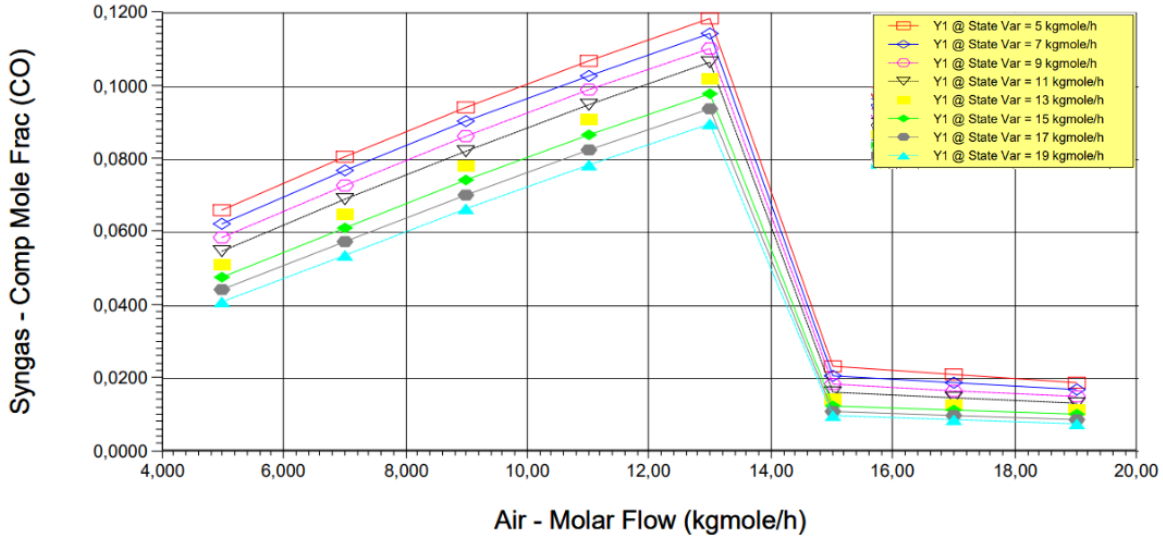


Figure 16 - Olive pit carbon monoxide composition (mass).

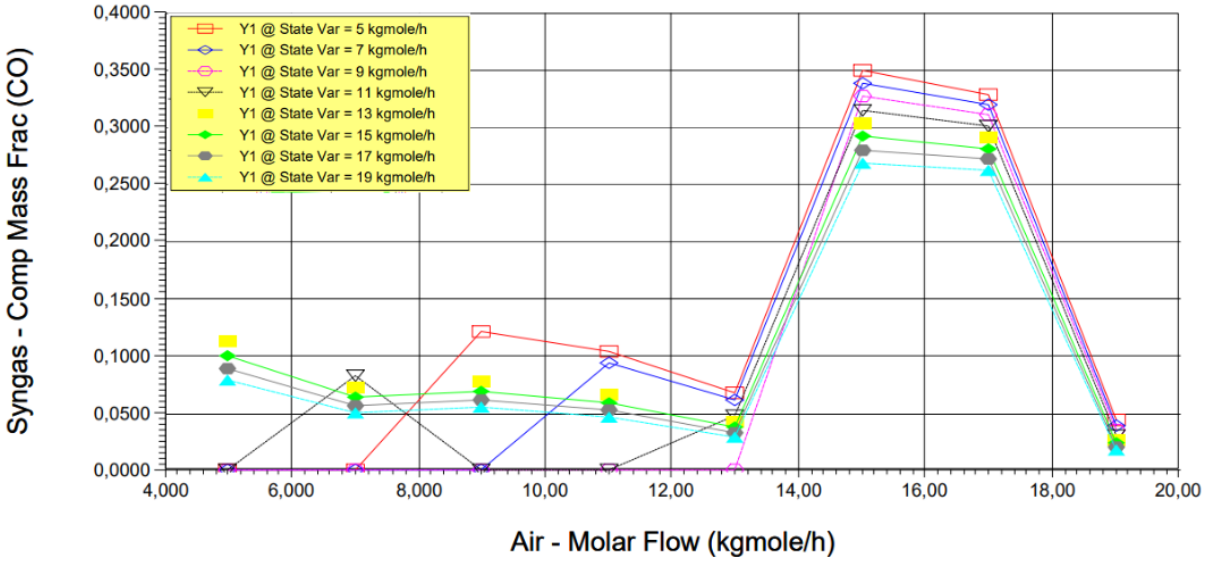


Figure 17 - Wood residue carbon monoxide composition (mass).

Analyzing the graphs, it is possible to perceive a different behavior between the different sources of biomass. For olive pit the increase in the flow of steam causes the composition of carbon monoxide to decrease, while for wood residue the vapor flow varies the composition between 5 and 13 kgmol/h and after that the vapor flow disfavors the formation of carbon monoxide. In the case of airflow, for olive pit the increase of air flow favors the formation of carbon monoxide up to approximately 13 kgmol/h and after that the formation decays a lot. In the case of olive pit the higher composition of carbon

makes total sense with a higher production in the end and then a decay after the most part of carbon has reacted. For wood residue the formation of carbon monoxide varies up to 13 kgmol/h and after that increases and decreases again passing 15 kgmol/h of air, a pattern similar with the olive pit but due to the different carbon composition and more moisture content the the pattern is not the same.

Franco et al. (2003) carried out the gasification process at 800°C and obtained reasonably different results for the carbon monoxide formation process, obtaining values between 0.35 and 0.3 for a steam/biomass ratio equal to 0.8, in the case of the present study the formation values are between 0 and 0.13, since the way the steam flow influences the values is the same as in the present study, lower vapor flows favor the formation of carbon monoxide, similar results were also reported by Usmani et. al. (2020).

### 4.2.2 Carbon dioxide

Figures 18 to 21 summarize the study of the influence of the variation of air and vapor inlet flows on the composition of carbon dioxide in the synthesis gas.

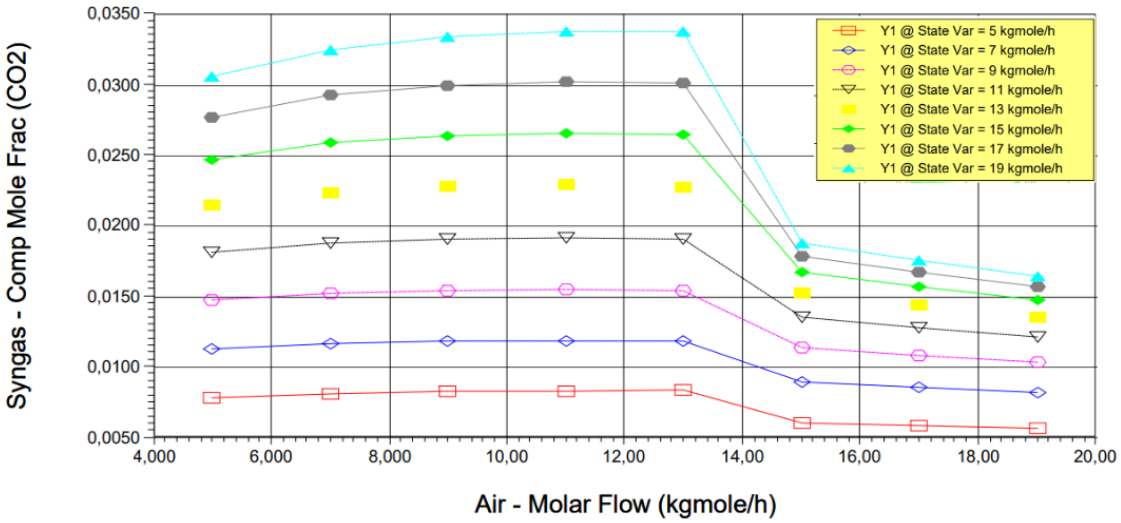


Figure 18 - Olive pit carbon dioxide composition (mole).

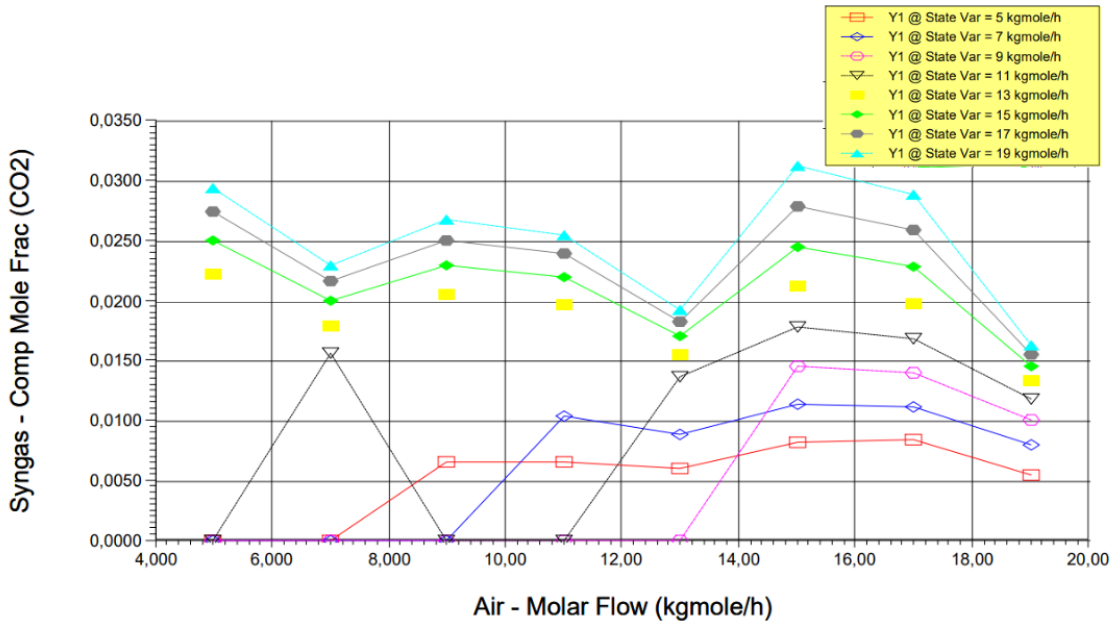


Figure 19 - Wood residue carbon dioxide composition (mole).

And represented in mass fractions:

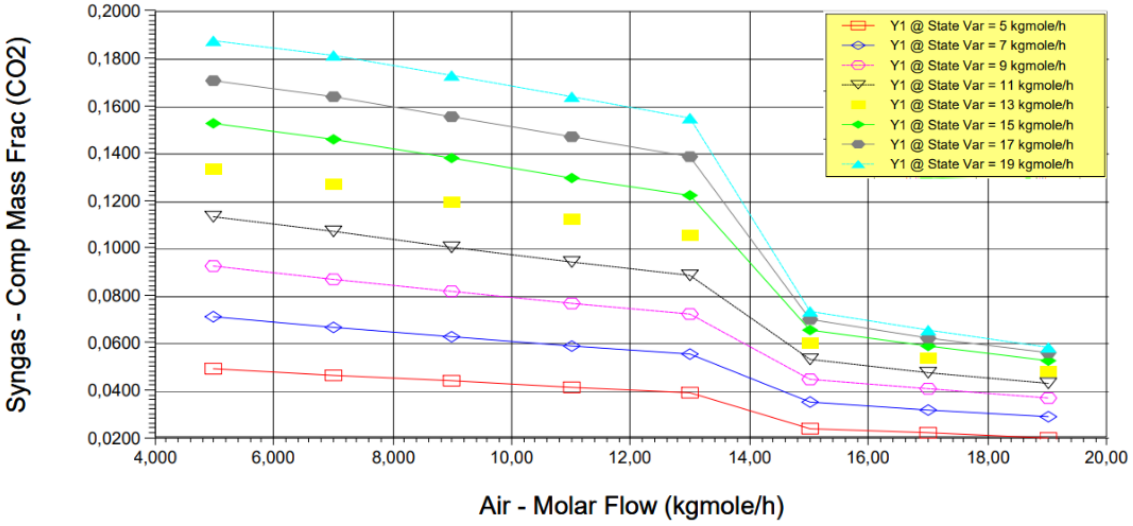


Figure 20 - Olive pit carbon dioxide composition (mass).

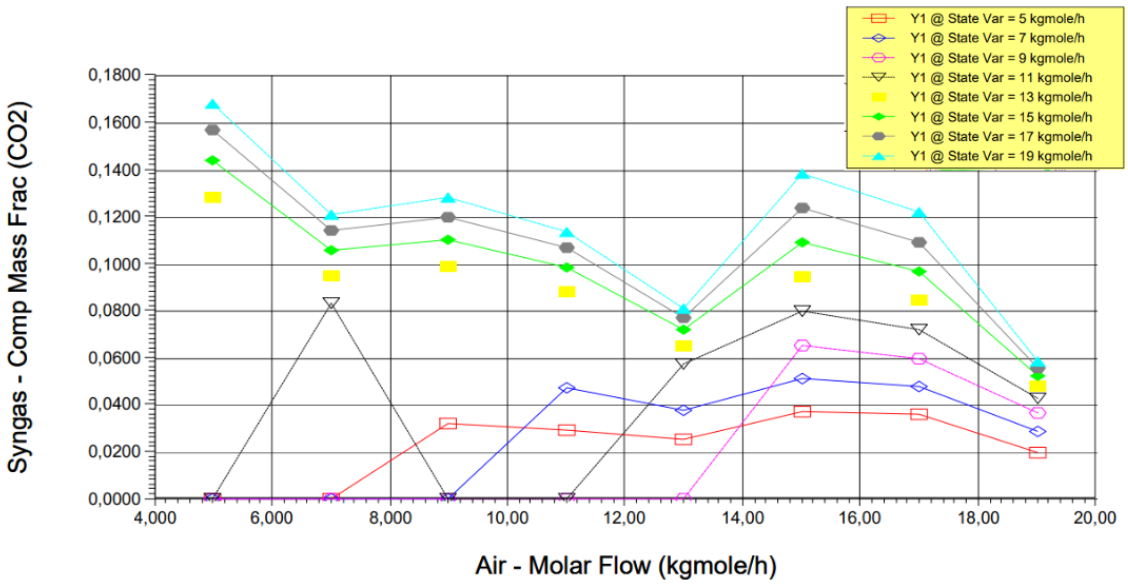


Figure 21 - Wood residue carbon dioxide (mass).

From the data it is possible to notice that the increase in the flow of steam in the case of olive pit increases the formation of carbon dioxide, and the increase in airflow decreases the formation of such a product. In the case of wood residue, the pattern is more difficult to predict, up to 11 kgmol/h of steam the composition of carbon dioxide varies greatly and for air flows of up to 15 kgmol/h the formation of carbon dioxide also varies significantly. For the other flow values, the increase in steam and air flows causes the decrease in formation to some extent and after that there is an increase followed by a decrease. This occurs due the higher presence of boudoard-reactions in later steps of the process.

### 4.2.3 Methane

The next composition studied was methane. In Figures 22 to 25 the influence of the variation of the vapor and water flows in the methane composition of the synthesis gas is showed.

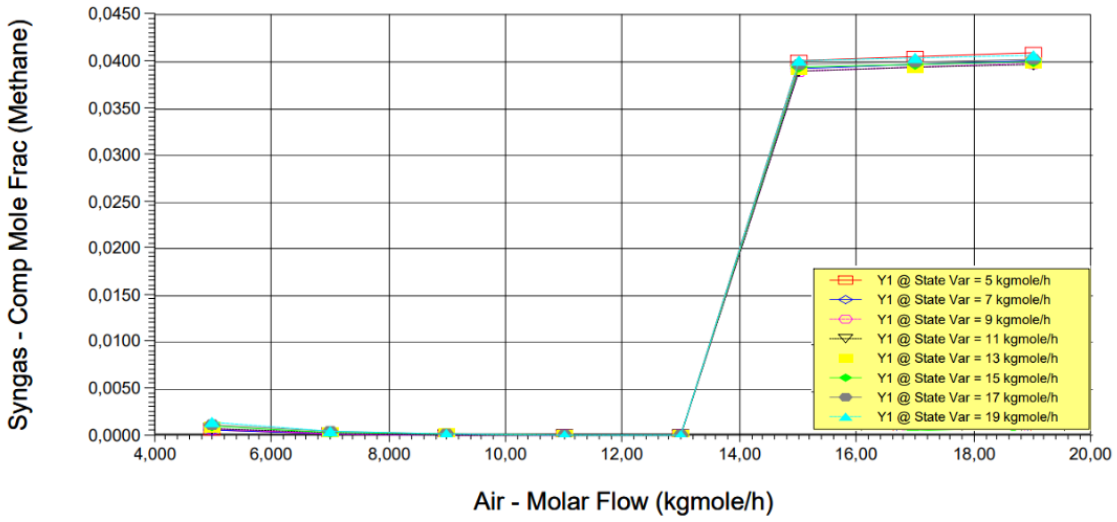


Figure 22 - Olive pit methane composition (mole).

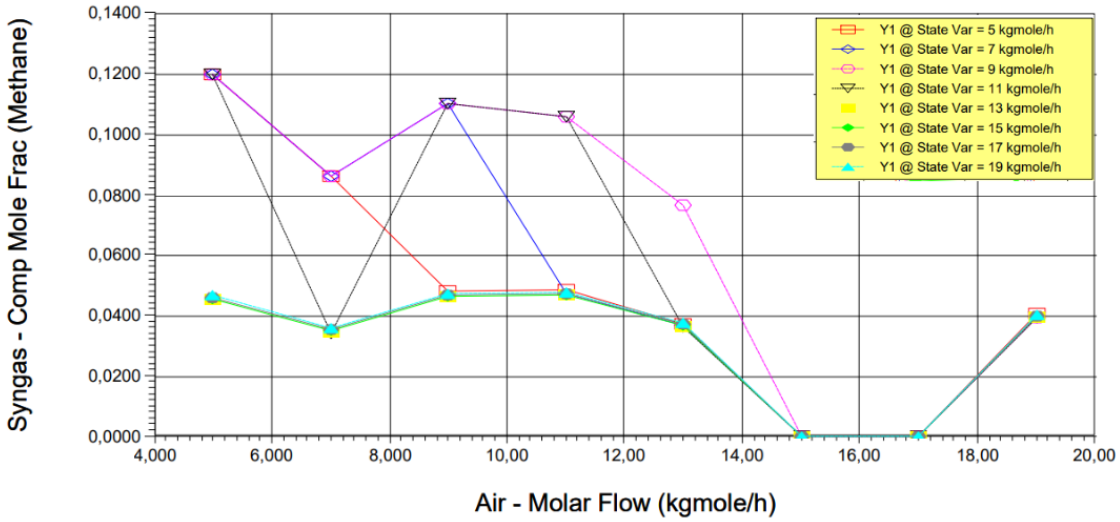


Figure 23 - Wood residue methane composition (mole).

And in mass fractions:

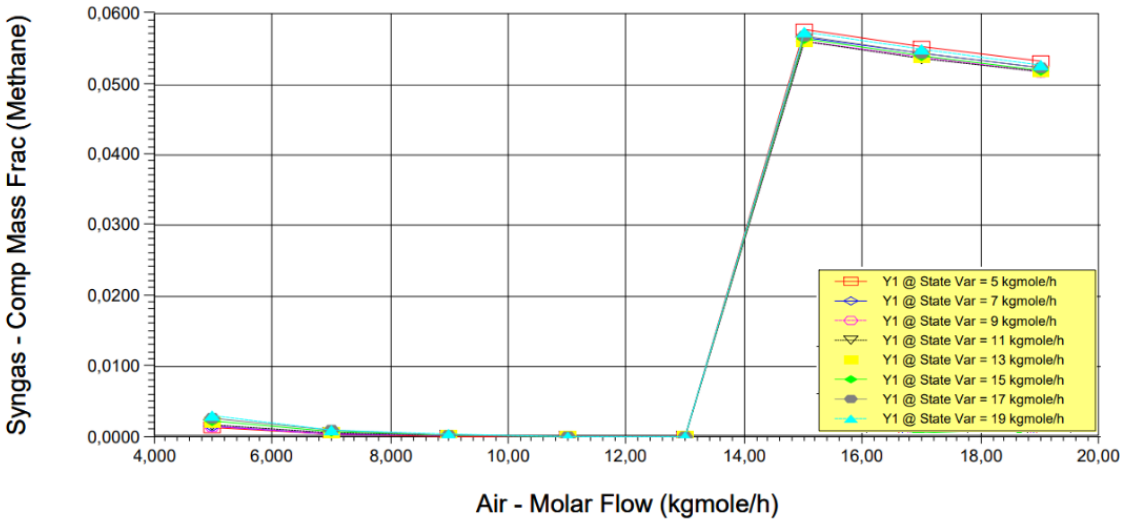


Figure 24 - Olive pit methane composition (mass).

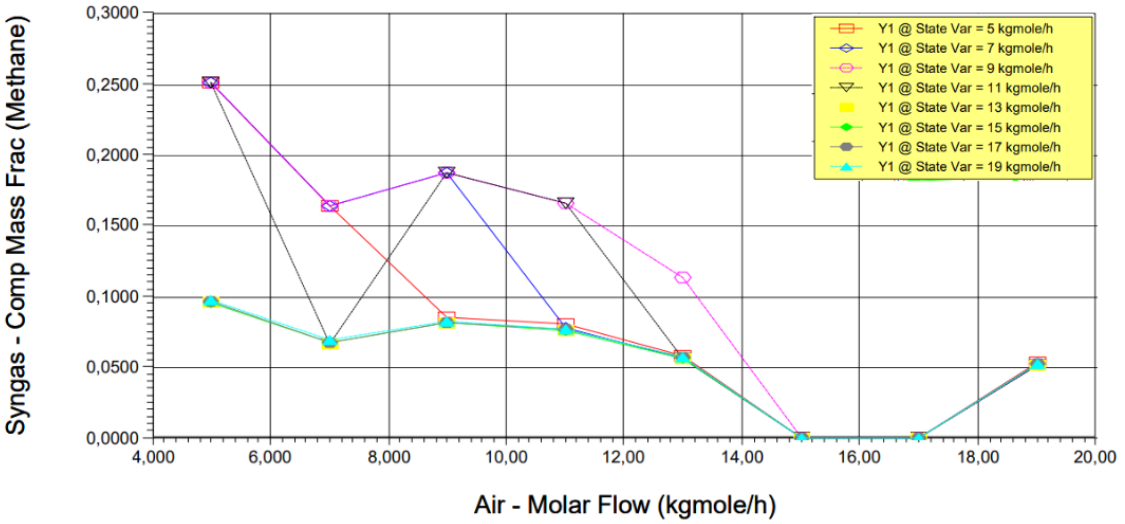


Figure 25 - Wood residue methane composition (mass).

Methane composition was the first major difference in curve behavior pattern due to its origin. In the case of olive pit methane formation increases with increased airflow and steam, while in the case of wood residue methane formation decreases up to 17 kgmol/h of air and grows back after that.

### 4.2.4 Hydrogen

Next, Figures 26 to 29 represent the influence of the variation of vapor and air flows in the hydrogen composition of the synthesis gas.

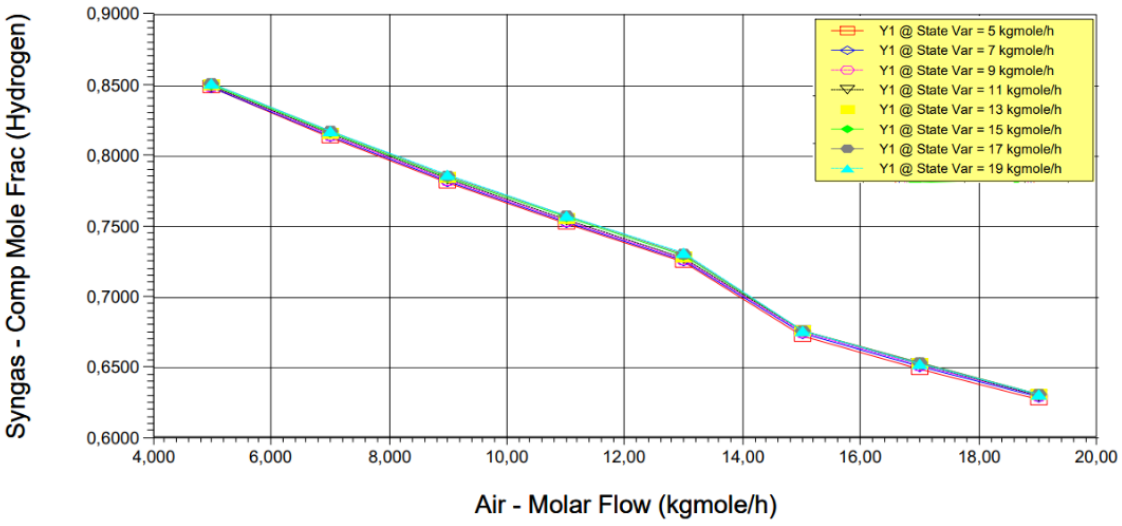


Figure 26 - Olive pit hydrogen composition (mole).

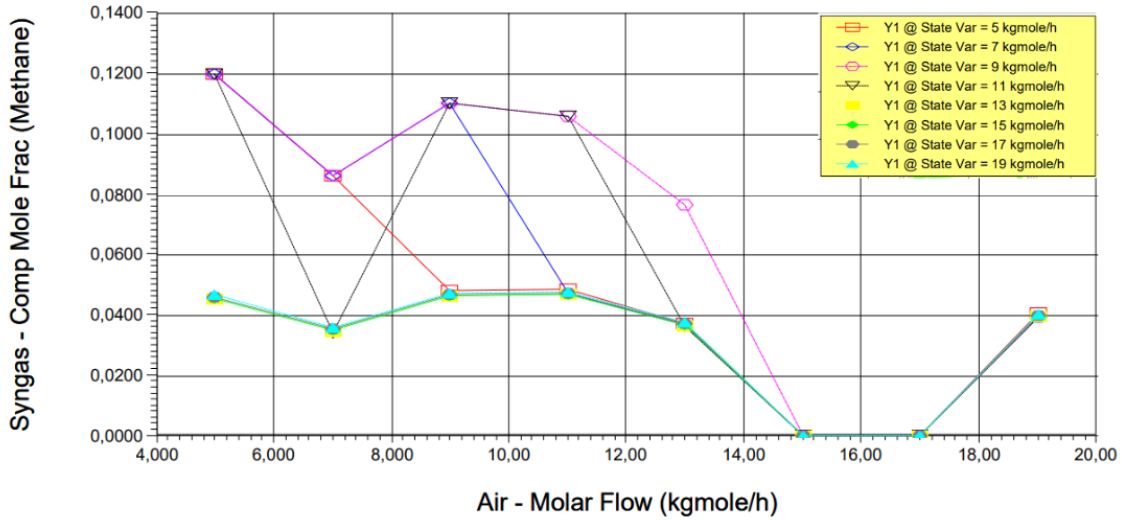


Figure 27 - Wood residue hydrogen composition (mole).

And in mass fractions:

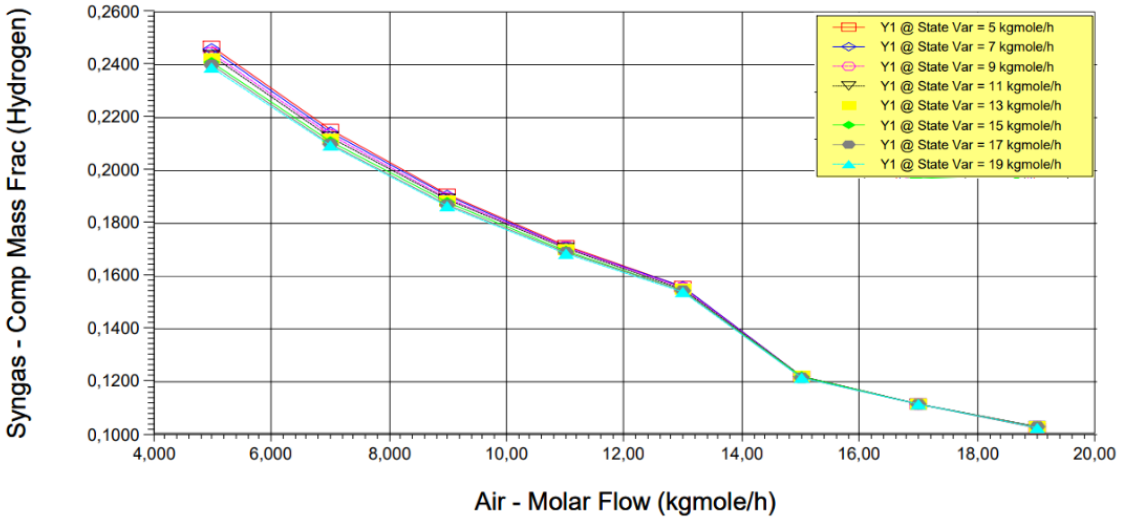


Figure 28 - Olive pit hydrogen composition (mass).

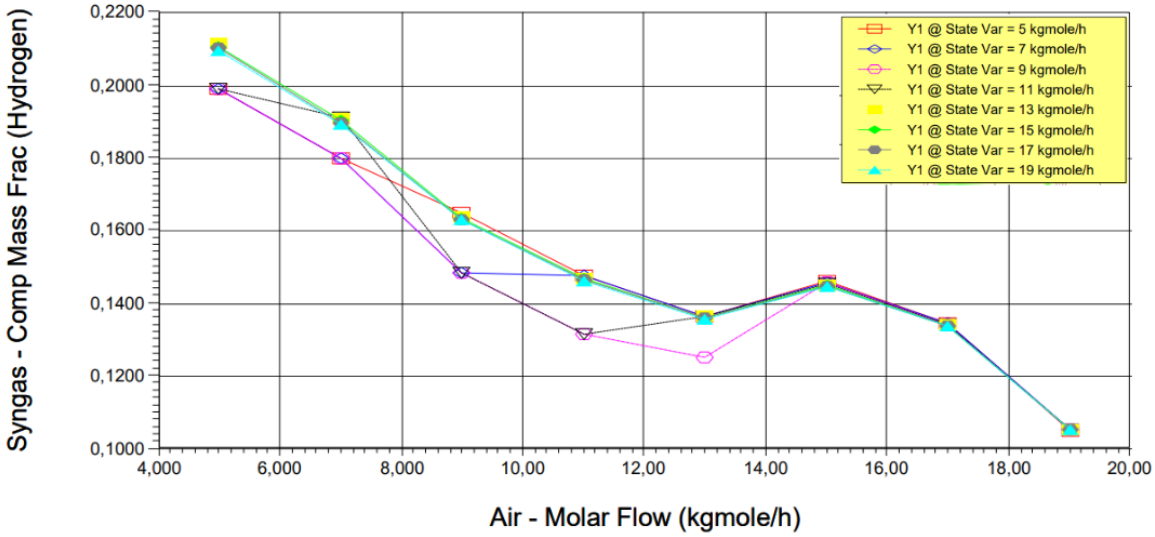


Figure 29 - Wood residue hydrogen composition (mass).

For hydrogen gas the behavior remained linear, for olive pit and wood residue the increase in air and vapor flows leads to decreased hydrogen gas formation, however this is still the majority product. For wood residue the value of steam flows influenced to some extent in a nonlinear way. Franco et al. (2003) obtained similar results by studying

the composition of syngas with a gasification at 800°C, for a 0.5 steam/biomass ratio he obtained $H_2$ formations close to 0.5 pair biomass from pine, in the case of the present study this ratio is repeated for air flows greater than 10 kgmol/h.

## 4.3 Temperature effect on syngas composition

In this stage the influence of the molar flow of steam added along with the influence of the steam temperature on the composition of the syngas will be analyzed. The following are represented the isotherms of the composition of the syngas as a function of the molar flow of steam, in this stage the molar flow of raw biomass is 10 kgmol/h.

The flow of steam was varied from 10 kg/h to 40 kg/h while maintaining air flow constant at 10 kg/h, which result in a steam/biomass ratio from 1.0 to 4.0. The focus of the study is mole fractions of CO, $CO_2$, $CH_4$ and $H_2$ as a function of steam/biomass ratio where are the different reaction temperatures for high-temperature gasification reactions temperatures vary from 600ºC to 1200ºC. This temperature range corresponds to the current gasification research/industrial implementation involving high-temperature gasification preferred. Usually, the temperature of wood gasification is below 800°C to 1000°C. However, with the inflow of high-temperature steam, the temperature of the reactor will increase, resulting in a higher reaction temperature. In addition, syngas components were evaluated to determine the viability of the concept with a relatively high response temperature.

The results exhibited that increasing the steam/biomass ratio had a significant effect on both components. At each given gas flow rate, the mole fractions of CO and $H_2$ showed opposite trends with increasing steam/biomass ratio. The mole fraction of CO shows a quadratic response (concave upward), with a minimum at the high-temperature gasification stage as a function of temperature. The minimum mole fraction of CO increases and moves upward with the increase of temperature in the high-temperature gasification stage steam/biomass ratio. For $H_2$ from residual wood biomass, a quadratic response (concave) was observed. As the temperature in the high-temperature gasification stage increases, the maximum mole fraction of $H_2$ decreases and shifts towards higher steam/biomass ratios. However, the behavior of olive pit biomass in relation to the formation of $H_2$ was different from that observed for wood residue. The results of the

present study were also reported by Usmani et al. (2020) that carried out the gasification process on hardwood chips.

After reaching a certain steam/biomass ratio, the trend reverses, $H_2$ production increases and CO production decreases as the ratio increases. However, depending on the water gas shift reaction, the steam/biomass ratio used for the shift varies at different gasification temperatures. The water gas shift reaction also produces carbon dioxide; however, this increase occurs for a given steam/biomass and gasification temperature. As reported by Pala et al. (2017). As $CO_2$ production increases, $CO_2$-consuming reactions such as the Boudouard reaction become dominant, leading to increased $CO_2$ production in steam reforming reactions.

### 4.3.1 Steam temperature effect on olive pit biomass

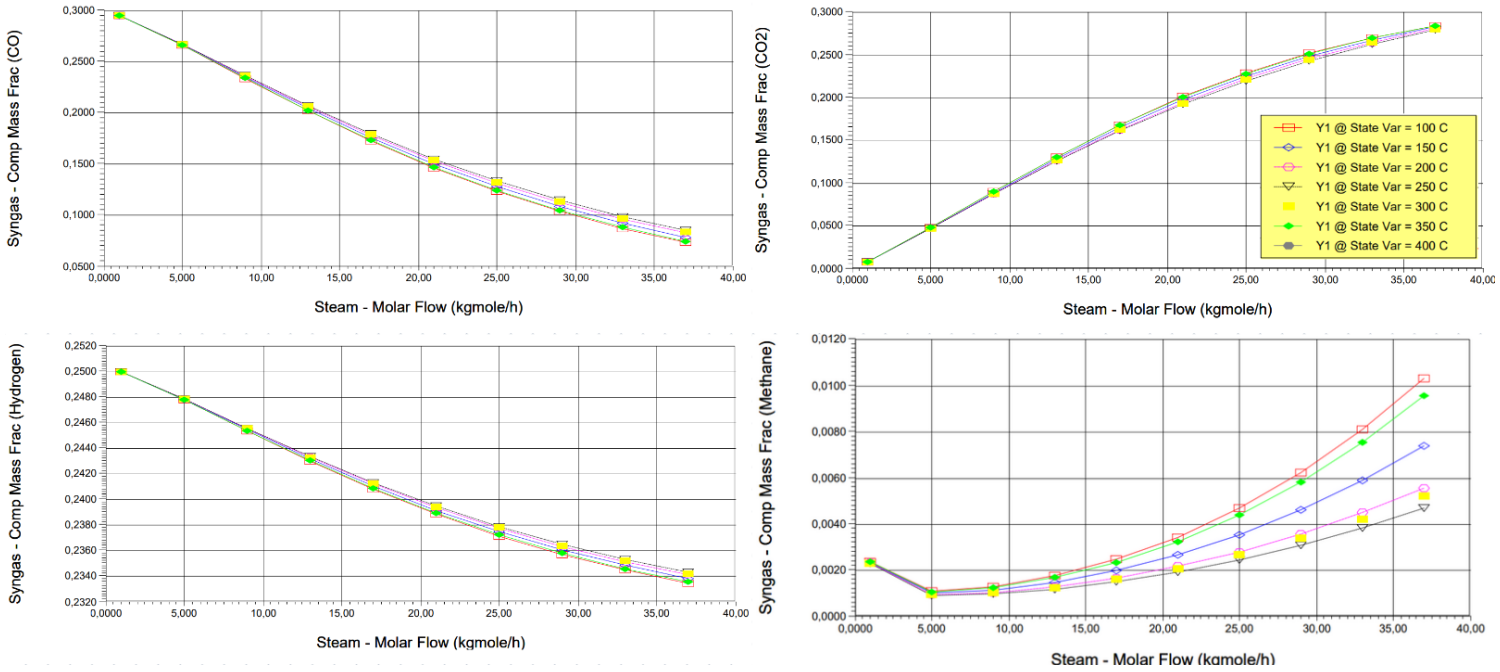


Figure 30 - Steam temperature effect on olive pit biomass.

Analyzing the curves (see Figure 30), it is possible to affirm that the temperature has a greater influence on methane formation than other products, with higher formation close to 100°C and lower formation close to 250°C.

Usmani et al. (2020) conducted a study on the composition of synthesis gas from hardwood biomass. In this study it also varies the flows and temperatures of the steam

current. In the case of the model shown in this work the influence is more significant because the addition of steam is directly in the reactors that perform the reduction, in the case of the present study the influence of steam is lower because in addition to the external vapor current, which has controlled parameters, the vapor cycle current from the pyrolysis separator also has influence. The present study obtained similar values of behavior, the increase in temperature favors the formation of hydrogen and carbon monoxide and the increase in vapor flow disfavors the formation of carbon monoxide and hydrogen, similar results, although in the case of Usmani et al. (2020) the studies were conducted with higher steam inlet temperatures (600 - 1200°C). This similar effect was also reported by Bermudez et al. (2016), Pindoria et al. (1998) and Franco et al. (2003).

### 4.3.2 Steam temperature effect on wood residue biomass

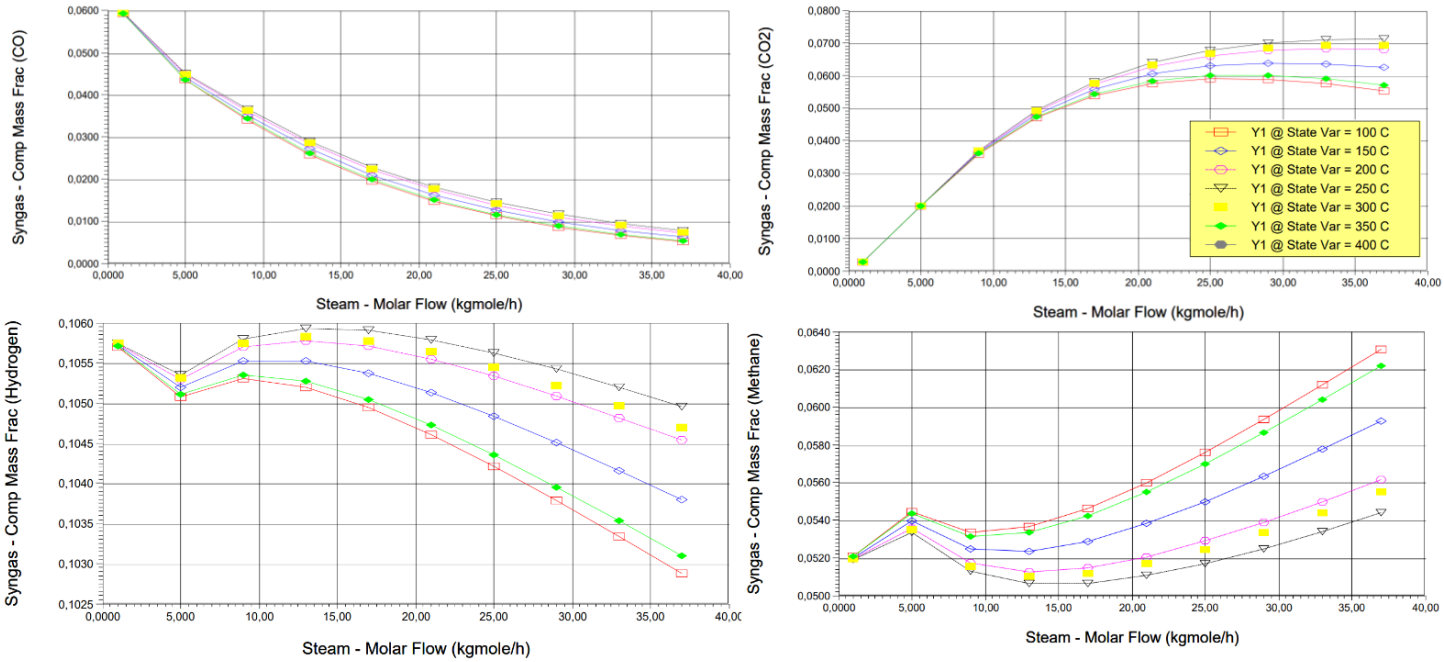


Figure 31 - Steam temperature effect on wood residue biomass.

In the case of the wood residue (see Figure 31), it is perceived that temperature has greater influence, being significant in the formation of carbon dioxide, methane, and hydrogen gas. The temperature being 250°C the one with the highest hydrogen yield. Methane and hydrogen isotherms exhibit unexpected behavior before a flow of 5 kgmol/h

of steam, also differing from the behavior pattern of olive pit curves, this may be due to some convergence error in the calculation of some results.

Using wood residue as a source of biomass, the behavior pattern of the curves was more faithful to the result observed by Usmani et al. (2020), Bermudez et al. (2016), Pindoria et al. (1998) and Franco et al. (2003). While for olive pit the hydrogen formation curves in the present study had linear behavior, for wood residue the behavior closely resembles a hyperbola, growing to a certain extent and after that decreasing, a pattern of behavior very similar to that observed by Usmani et al. (2020). In this case the temperature change is more significant, this is due to the different composition of biomass, with different carbon and humidity rates.

### 4.3.3 Energetic study

In this chapter, the study of temperature variation and heating heat required to achieve such conditions was carried out. It is worth remembering that the standard situation (the one where most composition studies were conducted, the reactors were considered adiabatic.

#### *4.3.3.1 Combustion*

To carry on with development of the study, the energy required for combustion was studied, the temperature of the reactor (state var) was varied according to the air inlet temperature.

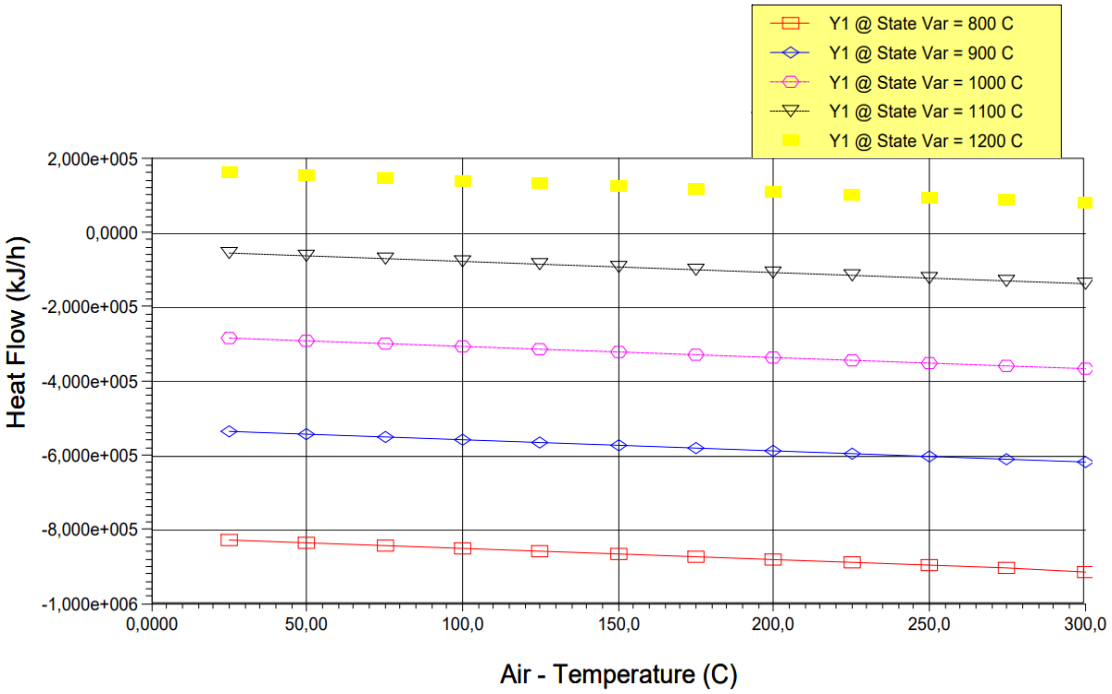


Figure 32 - Olive pit combustion heat flow.

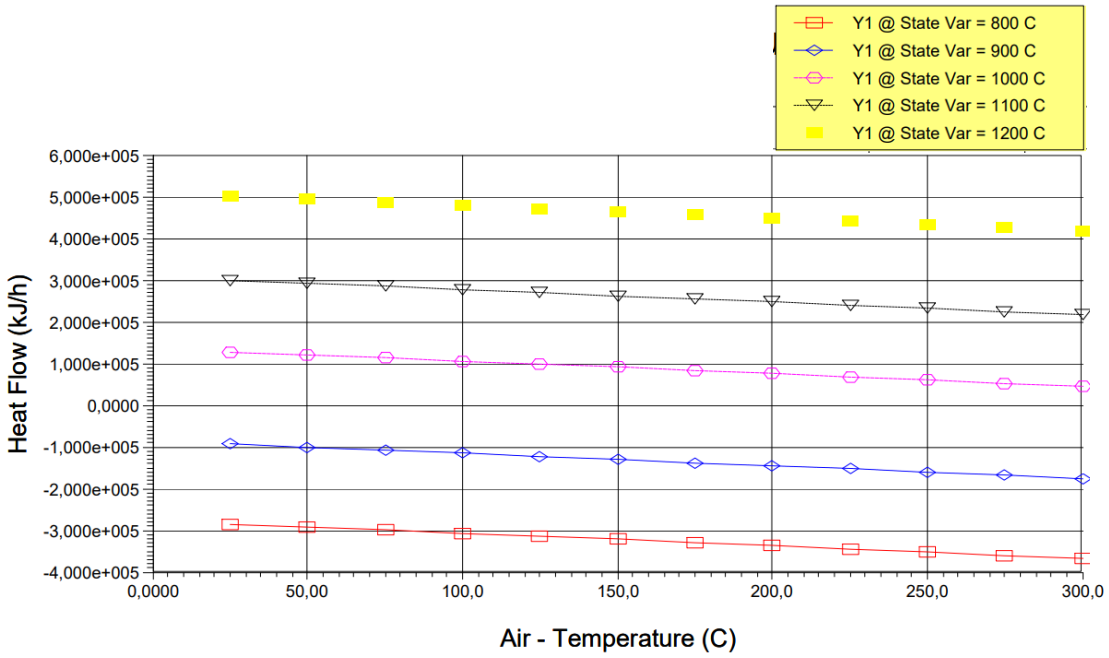


Figure 33 - Wood residue combustion heat flow.

From the observed data (see Figures 32 and 33) it is possible to infer that the air inlet temperature is very little influential in the heat required inside the equipment. It is noticed that the biomasses presented very different results, and the combustion reactions are exothermic until a certain temperature. In the case of olive pit, it is only necessary to

add energy from temperatures higher than 1100 °C, already for wood residue from approximately 950 °C it is already necessary to add heat.

### *4.3.3.2 Gasification*

Then the energy required for gasification was studied, the temperature of the reactor (state var) was varied according to the steam inlet temperature.

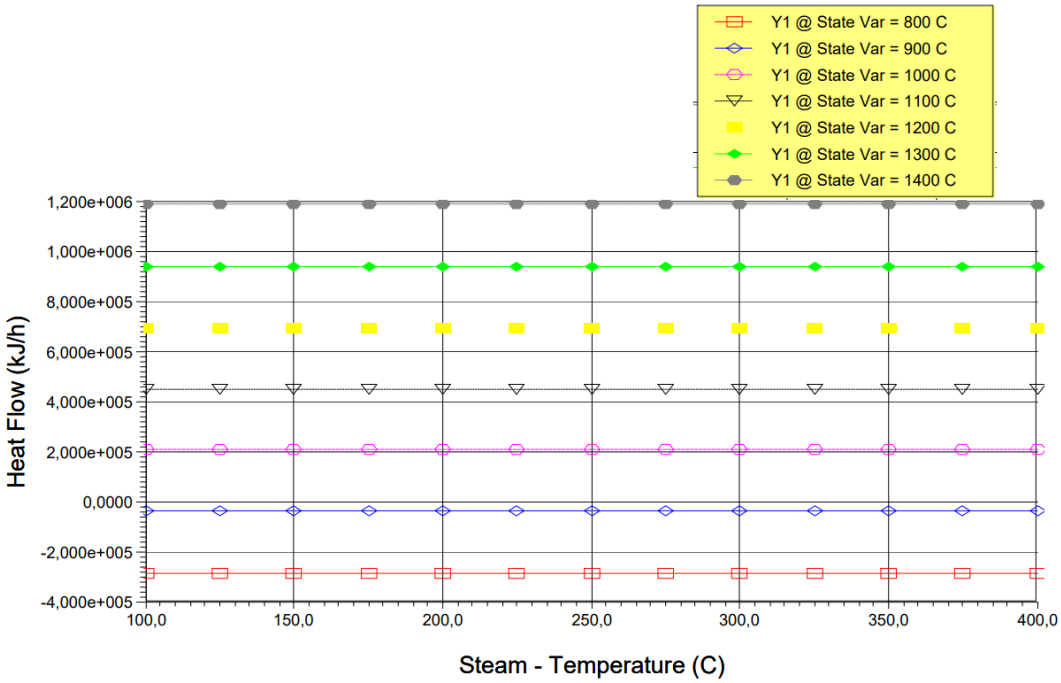


Figure 34 - Olive pit gasifier heat flow.

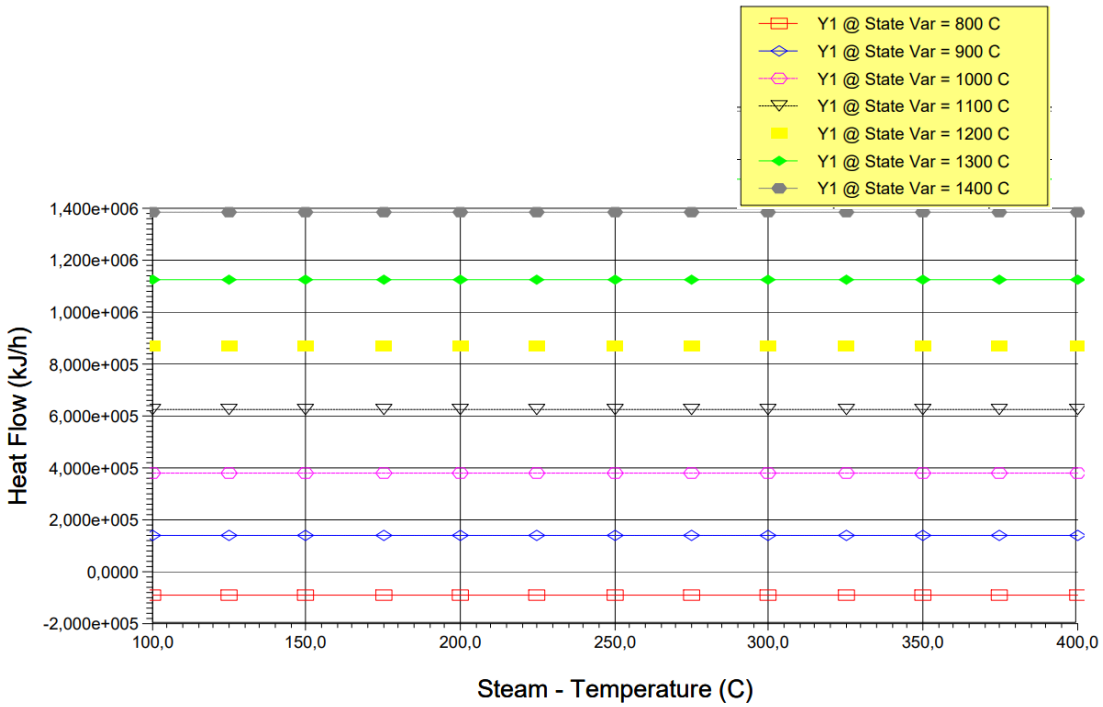


Figure 35 - Wood residue gasifier heat flow.

Like the air stream, the temperature of the steam current was not very influential in the gasification process (see Figures 34 and 35). Varying the temperature of the gasification reactors it is noticed that in the case of olive pit the reaction is exothermic to a certain extent, due to the fact of the temperature of the current coming from combustion, at temperatures up to approximately 900°C, and for wood residue the same happens only that the temperature where the reaction is exothermic is lower.

# *Part 5 - Conclusion and future works*

## 5.1 Conclusion

Using the kinetic model integrated with thermodynamic model it is possible to conclude that the results were satisfactory in the interval of 100 to 1500 K. The kinetic model presented a very similar behavior to those reported in the literature (Srivastava et al., 1996; Babu and Charausia, 2003; Koufopanos and Papayannakos, 1991). But this model does not separate the components specifically in its species ($CH_4$, $H_2$ CO, $CO_2$ and others), this model only separates the components into phases, in the case solid and gaseous, but for the software to understand the composition it is necessary to separate them into components ($CH_4$, $H_2$ and etc.), for this purpose using the thermodynamic model with a polynomial regression of data from the literature it was possible to separate the components in the pyrolysis stage (Neves et al.. 2011; Ahmad et al, 2016; Trninić et al., 2020). However, the thermodynamic model did not present consistent data at temperatures above 1200 K, because it is a model based on second-order equations, leading in certain cases to the formation of negative fractions of products, which was forcibly corrected. Another result is that was possible to confirm that the lower heating rates result in longer time for conversion to occur, and it was also possible to observe that the program from 25 seconds and lower heating rates does not have the expected behavior, leading to impossible results, such as negative mass fractions, pattern observed in the literature (Srivastava et al., 1996; Babu and Charausia, 2003; Koufopanos and Papayannakos, 1991). To finish the pyrolysis stage the mass balance of carbon, sulfur and water was significant to continue the process.

With the model developed it was possible to verify that the biomass composition interferes in the pyrolysis and gasification process. The mass balance led to different results of synthesis gas formation later. The simulation model does not have a previous drying of biomass precisely to verify whether the moisture content would be very influential in the formation of the product, and indeed it was, because higher moisture content was more susceptible to temperature influence and higher carbon biomass composition leaded to more methane and carbon monoxide and dioxide products.

The use of a recycle current increased the process yield because the kinetic model considers that the complete conversion of biomass does not occur. The biomass with higher moisture content (wood residue) was more susceptible to temperature influence than biomass with lower moisture content (olive pit). Wood residue generated

higher hydrogen and methane formation, as reported in the literature (Usmani et al., 2020; Bermudez et al., 2016; Pindoria et al., 1998; Franco et al, 2003).

Increasing the temperature and steam inlet favors the formation of $H_2$, CO and $CO_2$ while decreasing methane formation, other products ($C_xH_y$, $O_2$) are formed, but their behavior was not monitored. Increased steam flow results in increased formation of $CO_2$ and $H_2$, and increased airflow decreases the formation of these products. The increase in steam flow decreases the formation of $CH_4$ and CO, this occurs due to the higher occurrence of water-gas shift and Boudoard reactions (Franco et al., 2003).

The energy study determined that even varying the temperature of the air and steam inlet currents the determining factor for the energy demand of the reactors is the reactor temperature, in the case of combustion it is mostly exothermic and for gasification is mostly endothermal. So, if gasification is performed at a lower temperature (around 800°C, for the types of biomasses studied), the energy demand of the aerator is lower, which is logical, but decreases the yield of the studied products.

## 5.2 Future works

- It is possible to perform the improvement of the developed model; a possible alternative is to change the thermodynamic model adopted so that the composition of biomass can be more significant, adopting not only carbon, water and sulfur balance but other elements too, and it addresses a greater temperature range.
- The simulation model developed can be more energetically sustainable, using the current and energy generated by combustion in other stages of the process.
- The treated water can be reused for steam production, integrating the current into a vaporization process and after this is integrated the simulation plant.
- The formation of other products can be monitored to further improve studies, by the case study section in the software.

*References*


Ahmad, A. A. et al. **"Assessing the gasification performance of biomass: A review on biomass gasification process conditions. optimization and economic evaluation."**. Renew. Sustain. Energy Rev; (2016).

Andrade. R. V. "**Gaseificação de Biomassa: Uma Análise Teórica e Experimental"**; Universidade Federal de Itajubá; Instituto de engenharia mecânica - Programa de pós-graduação em engenharia mecânica. Itajubá. (2007).

Aranda G. Grootjes A. Van der Meijden C. Van der Drift A. Gupta D. Sonde R. et al. **"Conversion of high-ash coal under steam and $CO_2$ gasifcation conditions."** Fuel Process Technol; (2016).

Aravind S. Kumar P.S. Kumar N.S. Siddarth N. **"Conversion of green algal biomass into bioenergy by pyrolysis. A review".** Environ Chem. Lett. 18. 829–849. (2020).

Babich I., Hulst M. Lefferts L., Moulijn J., O'Connor P., Seshan K. **"Catalytic pyrolysis of microalgae to high-quality liquid biofuels"**. Biomass and Bioenergy. (2011).

Babu. B. V., and A. S. Chaurasia. **"Modeling. simulation and estimation of optimum parameters in pyrolysis of biomass"**. Energy Conversion and Management 44. Vol 13. 2135–58. (2003).

Basu, P., **"Biomass Gasification, Pyrolysis and Torrefaction: Practical Design and Theory,"** Biomass Gasification, Pyrolysis Torrefaction Pract. Des. Theory, pp. 1-530, second edition, (2013)

Bermudez, J.M. **"Handbook of Biofuels Production || Production of bio-syngas and bio-hydrogen via gasification".** (2016), 431–494.

Bryers R. W. **"Fireside slagging. fouling and high-temperature corrosion of heat transfer surface due to impurities in steam raising fuels."** Prog Energ Combust Sci. 22:29–120; (1996).

Buragohain. B., Mahanta. P., & Moholkar. V. S. **"Thermodynamic optimization of biomass gasification for decentralized power generation and Fischer–Tropsch synthesis".** Energy. 35(6): 2557–2579. (2010).

Campanella A., Harold M., **"Fast pyrolysis of microalgae in a falling solids reactor: Effects of process variables and zeolite catalysts".** Biomass and Bioenergy. 46. 218-232. (2012).

Castanheira. D. F. **"Estudo de um sistema de gaseificação para cogeração estudo experimental e de aplicação."** Dissertação de mestrado. Porto. (2017).

Chen S., Zhao Z., Soomro A., Ma S.. Wu M., Sun Z., Xiang W., **"Hydrogen-rich syngas production via sorption-enhanced steam gasification of sewage sludge."** Biomass and Bioenergy. (2020).

Cunha. J., A. M. **Caracterização das cadeias de abastecimento de biomassa florestal em Portugal**. INESCTEC. Porto. (2019).

Das P., Chandramohan V.P., Mathimani T., Pugazhendhi A., **"A comprehensive review on the factors affecting thermochemical conversion efficiency of algal biomass to energy."** Science of The Total Environment. (2021).

Demirbas. A. "**Combustion characteristics of different biomass fuels."** Prog Energ Combust Sci. 30:219–30; (2004).

Fernandes. E. R. K. **"Valorização de resíduos gerados na bananicultura por conversão termoquímica por pirólise."** Dissertação (Mestrado em Engenharia de Processos). Universidade da Região de Joinville. UNIVILLE. (2012).

Franco, C.; Pinto, F.; Gulyurtlu I.; Cabrita, I. **"The study of reactions influencing the biomass steam gasification process".** (2003), 82(7), 835–842.

Funabashi. T.**; Integration of Distributed Energy Resources in Power Systems**; Institute of Materials and Systems for Sustainability (IMaSS). Nagoya University. Nagoya. Japan. (2016).

He Q., Guo Q., Umeki K., Ding L., Wang F., Yu G., **"Soot formation during biomass gasification: A critical review."** Renewable and Sustainable Energy Reviews. (2021).

Janajreh I., Adeyemi I. Raza S. S., Ghenai C. **"A review of recent developments and future prospects in gasification systems and their modeling".** Renewable and Sustainable Energy Reviews. (2021).

Khan. A. A., Jong. W., Jansensrg. P.J., Spliethoff. H., **"Biomass combustion in fluidized bed boilers: Potential problems and remedie**s". Fuel Processing Technology. Vol.90 21-50; (2008).

Koufopanos C. A., **"Modelling of the Pyrolysis of Biomass Particles. Studies on Kinetics. Thermal and Heat Transfer Effects ".**The Canadian J Chem. Eng. (1991).

Laurichesse. S.; Avérous. L. **"Chemical modification of lignins: towards biobased polymers.** ***Progress in Polymer Science***". v. 39. n. 7. p. 1266-1290; (2014).

Lin, W.; Lester, O. P.; Agus, H.; James, W. **"Co-gasification of hardwood chips and crude glycerol in a pilot scale downdraft gasifier."** (2011), 102(10), 6266–6272.

Lisboa. F.. **"Carbonização e gaseificação de resíduos da macaúba. tucumã e cupuaçu para geração de eletricidade."** Dissertação. universidade de Brasília. Brasília. (2016).

Loo. S.V. Koppejan. J. **"The Handbook of Biomass Combustion & Co-firing"**. London: Earthscan. cop. (2008).

Mahamulkar S., Yin K., Agrawal PK., Davis RJ., Jones CW., Malek A., et al. **"Formation and oxidation/gasifcation of carbonaceous deposits: a review".** Ind Eng Chem Res. (2016); 55:9760–818.

Maldonado, P. A. F., **"Biomass gasification processes - modeling and simulation".** Escola Superior de Tecnologia e Gestão of the Instituto Politécnico de Bragança. (2022).

Maniscalco, M., Paglia, F., Iannotta, P., Caputo, G., Scargiali F., Grisafi F., Brucato A., **"Slow pyrolysis of an LDPE/PP mixture: Kinetics and process performance".** Journal of the Energy Institute. (2021).

Masia, A. A. T., Buhre B. J. P. Gupta R. P. Wall T. F. **"Characterising ash of biomass and waste."** Fuel Process Technol. (2007); 88:1071–81.

McKendry, P., **"Energy production from biomass (part 1): overview of Biomass"**. Bioresource Technology. (2002a).

McKendry, P., **"Energy production from biomass (part 2): conversion technologies".** Bioresource Technology. (2002b).

McKendry, P., **"Energy production from biomass (part 3): gasification technologies.**" Bioresource technology. (2002c).

Mesquita. g. B. **"Gaseificação de biomassa fecal humana: análise do processo via aspen plus e estudo do gás de síntese como combustível em um motor de combustão interna."** Universidade federal do espírito santo. espírito santo. (2017).

Miles T. R., Miles J. T. R., Baxter L. L. Bryers R. W. Jenkins B. M., Oden L. L. "**Alkali deposits found in biomass power plants. A preliminary investigation of their extent and nature".** Report of the National Renewable Energy Laboratory (NREL/TZ-2-11226-1; TP-433-8142). Golden. CO. USA; (1995).

Mlonka-Mędrala A., Evangelopoulos P., Sieradzka M., Zajemska M., Magdziarz A., **"Pyrolysis of agricultural waste biomass towards production of gas fuel and high-quality char: Experimental and numerical investigations".** Fuel. 296. 120611. (2021).

Molino. A., Chianese. S., & Musmarra. D. **"Biomass gasification technology: The state of the art overview".** Journal of Energy Chemistry. (2016)

Molino. A., Larocca. V., Chianese. S., Musmarra. D. **"Biofuels production by biomass gasification: A review"**. Energies. (2018).

Neves. D., et. al. **"Characterization and prediction of biomass pyrolysis products."** Progress in Energy and Combustion Science. Vol 37. 611-630. (2011).

Nguyen T.S., He S., Raman G., Seshan K., **"Catalytic hydro-pyrolysis of lignocellulosic biomass over dual Na2CO3/Al2O3 and Pt/Al2O3 catalysts using n-butane at ambient pressure".** Chemical Engineering Journal. 299. 415-419. (2016).

Nikoo. M.B.; Mahinpey. N. **"Simulation of biomass gasification in fluidized bed reactor using ASPEN PLUS".** Biomass and Bioenergy. 32: 1245–1254 (2008).

Ningbo G., Baoling L., Aimin L., Juanjuan L. **"Continuous pyrolysis of pine sawdust at different pyrolysis temperatures and solid residence times".** Journal of Analytical and Applied Pyrolysis. 114. 155-162. (2015).

Paiva. M.; **"Modeling and simulation of a biomass gasification processes."** MSc. Thesis. Instituto Politécnico de Bragança. Bragança. (2020).

Pala, L.P.R., Wang, Q., Kolb, G., Hessel, V., **"Steam gasification of biomass with subsequent syngas adjustment using shift reaction for syngas production: An Aspen Plus model",** Renewable Energy. 101 (2017) 484–492

Peterson A.A., Vogel F., Lachance R.P., Fröling M., Antal M.J., J.W. Tester J.W., **"Thermochemical biofuel production in hydrothermal media: a review of sub- and supercritical water technologies".** Energy Environ. Sci. (2008).

Pindoria, R.V.; Megaritis, A.; Messenböck, R.C.; Dugwell, D.R.; Kandiyoti, R. **"Comparison of the pyrolysis and gasification of biomass: effect of reacting gas atmosphere and pressure on Eucalyptus wood."** (1998), 77(11), 1247–1251.

Quaak. P., Knoef. H., Stassem. H., **"Energy from biomass: a review of combustion and gasification technologies"**. Washington D.C.: The International Bank for Reconstruction and Development/The World Bank. cop. (1999).

Ramzan. N., Ashraf. A., Naveed. S., & Malik. A. **"Simulation of hybrid biomass gasification using Aspen plus: A comparative performance analysis for food. municipal solid and poultry waste"**. Biomass and Bioenergy. (2011); 35(9): 3962–3969.

RCM n.º 163/2017; Diário da República. 1.ª série; N.º 210; outubro de (2017).

Regueira. L.N., Añón. J.R., Castiñeiras. J.P. e Garcia. A.R. "**Energetic evaluation of biomass originating from forest waste by bomb calorimetry. Journal of Thermal Analysis and Calorimetry**.". (2001); 66: 281-292.

Rodrigues. D. M. **"Sistema de Produção de Hidrogénio através da Eletrólise da Água alimentado por um Aerogerador – Análise económica".** Instituto Politécnico de Bragança. Engenharia de Energias Renováveis. Bragança. (2019).

Rohman, F. S.; Sulaiman, S. H. S.; Aziz, N. **"Modelling and simulation of hydrogenation of dimethyl oxalate in ethylene glycol production".** IOP Conf. Ser.: Mater. Sci. Eng. 991 012140 (2020).

Sahoo S., Vijay V., Chandra R., Kumar H. **"Production and characterization of biochar produced from slow pyrolysis of pigeon pea stalk and bamboo".** Cleaner Engineering and Technology. (2021).

Saião. M. **"Implementação de uma central a biomassa - análise de sustentabilidade ambiental e económica".** Lisboa: Instituto Superior Técnico. Universidade Técnica de Lisboa. (2009). Tese de mestrado.

Srivastava V. K., Sushil. Jalan R.K. **"Prediction of concentration in the pyrolysis of biomass material—ii"** Energy Convers Manage. (1996).

Theis M. Skrifvars B-J. Hupa M. Tran H. "**Fouling tendency of ash resulting from burning mixtures of biofuels. Part 1: Deposition rates Fuel".** (2006); 85 :1125–30

Tool box, E., **"Combustion Heat," Resources, Tools and Basic Information for Engineering and Design of Technical Applications",** (2017)

Usmani, S.; Gonzalez Q. A.; Vasquez P., R.; Palmer, G.; Lake, M. **"Simulation model of the characteristics of syngas from hardwood biomass for thermally integrated gasification using unisim design tool".** Energy, 211; (2020).

Vamvuka D. Zografos D. **"Predicting the behaviour of ash from agricultural wastes during combustion".** Fuel. (2004); 83:2051–7.

Vassilev S., Baxter D., Andersen L., Vassileva C., "**An overview of the chemical composition of biomass**". Fuel. Vol.89 (2010) 913–933.

Vieira. G. E. G. et al.; **Biomassa: uma visão dos processos de pirólise**; Revista Liberato. Novo Hamburgo. (2014).

Wei X. Schnell U. Hein K. R. G**. "Behaviour of gaseous chlorine and alkali metals during biomass thermal utilisation."** Fuel. (2005).

Werther. J., Saenger. M., Hartge. E-U., Ogada T. Siagi Z. **"Combustion of agricultural residues"**. Prog Energ Combust Sci. (2000).

Zhang. H., Zhang. S., Weng. Z., Mubeen I., Zhang C., Yan M., Fauziah S.. **"Gaseificação de água supercrítica catalisada por álcali de lodo de esgoto: efeito da reutilização de resíduos líquidos como catalisador homogêneo".** Int. J. Environ. Sci. Technol. (2020).

## APPENDIX A – Pyrolysis Python Program

```
#biomass pyrolysis
import math
import pylab
from math import exp
import matplotlib.pyplot as plt
import numpy as np

#data

cperc=float(input('Insert Carbon percentage (%): '))
title = str(input('Insert graphs title: '))
umidity = float(input('Insert umidity (%): '))
sperc = float(input('Insert sulfur percentage (%): '))
mass = float (input("Insert mass flow (kg/h): "))
tempinitial = float(input("Insert initial temperature (K): "))
hr = float(input("Insert heating rate (K/s): ")) # K/s
tf = float(input("Considering initial time = 0, insert final time (s): ")) #s
```

```
#first mass balance calculations

c = cperc*10 #g
s = sperc/ 100
water = umidity/100#Kg

# mass composition

c_mass_i = c*mass
s_mass_i = s*mass
water_mass_i = water*mass

# molar mass
c_mm = 12 #g/mol
h_mm = 1 #g/mol
o_mm = 16 #g/mol
n_mm = 14 # g/mol
s_mm = 32# g/mol
water_mm = 2*h_mm + o_mm

#molar composition
c_mol_i = c_mass_i/c_mm #mol/h
s_mol_i = s_mass_i/s_mm #mol/h
water_mol_i = water_mass_i/water_mm #mol/h
```

```
#products molar masses:

#Liquids

benz_mm = 78 #g/mol
tol_mm = 92.14
naph_mm = 128.17

#gases

ch4_mm = 16 #g/mol
co_mm = 28
co2_mm = 44
h2_mm = 2

#char products
h20 = 18 #g/mol
n2_mm = 28
o2_mm = 32
```

```
# kinetic model parameters

a1 = 9.973*10**(-5) #s^-1
a2 = 1.068*10**(-3) #s^-1
a3 = 5.7*10** (5) #s^-1
d1 = 17254.4 #K
d2 = 10224.4 #K
l1 = -9061227 #K^2
l2 = -6123081 #K^2
e3 = 81*10**3 # kJ/mol
R = 8.314 # J/K.mol
h = 0.1
ti = 0 #s
n = int ((tf-ti)/h)
```

```
#ODE1 concentration of biomass (CB)

xCB_plot = []
yCB_plot = []
time_list = []
#Initial conditions

cb=1
t = 0

#RK 4th order method

for i in range(0,n):
        temp = hr*(t)+tempinitial
        k1 = a1*exp((d1/temp)+(l1/temp**2))
        k2 = a2*exp((d2/temp)+(l2/temp**2))
        k3 = a3*exp((-e3/(R*temp)))
        c1 = -k1*cb-k2*cb
        c2 = -k1*(cb+c1*h/2)-k2*(cb+c1*h/2)
        c3 = -k1*(cb+c2*h/2)-k2*(cb+c2*h/2)
        c4 = -k1*(cb+c3*h)-k2*(cb+c3*h)
        c = (c1+2*c2+2*c3+c4)*h
        cb = cb + 1/6 * c
        t=t+h

        xCB_plot.append(t)
        yCB_plot.append(cb)
        time_list.append(t)
```

```
#ODE2 concentration of gases 1 (CG1)

xG1_plot = []
yG1_plot = []

#Initial conditions

cg1=0.01
cb =1
cc1 = 0.01
t = 0

#RK 4th order method

for i in range(0,n):
        temp = hr*(t)+tempinitial
        k1 = a1*exp((d1/temp)+(l1/temp**2))
        k2 = a2*exp((d2/temp)+(l2/temp**2))
        k3 = a3*exp((-e3/(R*temp)))
        c1 = k1*cb- k3* cg1**1.5*cc1**1.5
        c2 = k1*cb- k3* (cg1+c1*h/2)**1.5*(cc1**1.5)
        c3 = k1*cb- k3* (cg1+c2*h/2)**1.5*cc1**1.5
        c4 = k1*cb- k3* (cg1*h)**1.5*cc1**1.5
        c = (c1+2*c2+2*c3+c4)/6*h
        cg1 = cg1 + 1/6 * c
        t=t+h

        xG1_plot.append(t)
        yG1_plot.append(cg1)
```

```
#ODE3 concentration of Char 1 (CC1)

xC1_plot = []
yC1_plot = []

#initial conditions

cg1=0.01
cb =1
cc1 = 0.01
t = 0

#RK 4th order method

for i in range(0,n):
        temp = hr*(t)+tempinitial
        k1 = a1*exp((d1/temp)+(l1/temp**2))
        k2 = a2*exp((d2/temp)+(l2/temp**2))
        k3 = a3*exp((-e3/(R*temp)))
        c1 = k2*cb- k3* cg1**1.5*cc1**1.5
        c2 = k2*cb- k3* (cg1+c1*h/2)**1.5*cc1**1.5
        c3 = k2*cb- k3* (cg1+c2*h/2)**1.5*cc1**1.5
        c4 = k2*cb- k3* (cg1*h)**1.5*cc1**1.5
        c = (c1+2*c2+2*c3+c4)/6*h
        cc1 = cc1 + 1/6 * c
        t=t+h

        xC1_plot.append(t)
        yC1_plot.append(cc1)
```

```
#ODE4 concentration of  gases 2 (G2)

xG2_plot = []
yG2_plot = []

#initial conditions

cg2 = 0.00001
cg1=0.01
cc1 = 0.01
t = 0

#RK 4th order method

for i in range(0,n):
        temp = hr*(t)+tempinitial
        k1 = a1*exp((d1/temp)+(l1/temp**2))
        k2 = a2*exp((d2/temp)+(l2/temp**2))
        k3 = a3*exp((-e3/(R*temp)))
        c1 = k3* cg1**1.5*cc1**1.5
        c2 = k3* (cg1+c1*h/2)**1.5*cc1**1.5
        c3 = k3* (cg1+c2*h/2)**1.5*cc1**1.5
        c4 = k3* (cg1*h)**1.5*cc1**1.5
        c = (c1+2*c2+2*c3+c4)/6*h
        cg2 = cg2 + 1/6 * c
        t=t+h

        xG2_plot.append(t)
        yG2_plot.append(cg2)
```

```
#ODE4 concentration of char 2 (C2)

xC2_plot = []
yC2_plot = []
temp_list = []
time_list = []
#initial conditions

cc2 = 0.00001
cg1=0.01
cc1 = 0.01
t = 0

#RK 4th order method

for i in range(0,n):

        temp = hr*(t)+tempinitial
        k1 = a1*exp((d1/temp)+(l1/temp**2))
        k2 = a2*exp((d2/temp)+(l2/temp**2))
        k3 = a3*exp((-e3/(R*temp)))
        c1 = k3* cg1**1.5*cc1**1.5
        c2 = k3* (cg1+c1*h/2)**1.5*cc1**1.5
        c3 = k3* (cg1+c2*h/2)**1.5*cc1**1.5
        c4 = k3* (cg1*h)**1.5*cc1**1.5
        c = (c1+2*c2+2*c3+c4)/6*h
        cc2 = cc2 + 1/6 * c
        time_list.append(t)
        temp_list.append(temp)
        t=t+h

        xC2_plot.append(t)
        yC2_plot.append(cc2)
```

```
#balance check
conversion_plot = []
for i in range(len(xCB_plot)):
    balance_check = yCB_plot[i]+yG1_plot[i]+yC1_plot[i]+yG2_plot[i]+yC2_plot[i]
    conversion = balance_check*100
    conversion_plot.append(conversion)
plt.plot(xCB_plot,conversion_plot)
plt.xlabel("Time (s)")
plt.ylabel("Conversion (%)")
```

```
# Ploting the results
plt.plot(xCB_plot,yCB_plot, label = "CB")
plt.plot(xG1_plot,yG1_plot, label = "CG1")
plt.plot(xC1_plot,yC1_plot, label = "CC1")
plt.plot(xG2_plot,yG2_plot, label = "CG2")
plt.plot(xC2_plot,yC2_plot, label = "CC2")
plt.title(title)
plt.xlabel("Time (s)")
plt.ylabel("Concentration")
plt.legend()
plt.show()
plt.title(title)
```

```
#defining gas and liquid separation
ygases = []
for i in range(len(temp_list)):

        ygas = (0.0001*(temp_list[i])**2 - 0.0817*(temp_list[i]) + 50.502)/200
        ygases.append(ygas)
```

```
#concentration of volatiles
volatiles = []
volatiles_mass = []

#Liquids

ynaph_list = []
naph_list_mass = []
ybenz_list = []
benz_list_mass = []
ytol_list = []
tol_list_mass = []


for i in range(len(yG1_plot)):
    sum_vol = yG1_plot[i]+yG2_plot[i] #volatiles fraction mass balance
    mass_sum_vol = sum_vol*mass #volatiles mass balance
    volatiles.append(sum_vol)
    volatiles_mass.append(mass_sum_vol)

    #liquid fractions
    sum_liq = (1-ygases[i])*volatiles[i] #Liquids fraction mass balance
    mass_sum_liq = sum_liq*mass #liquids mass balance

    ynaph = sum_liq*0.2
    if ynaph <0:
        ynaph = 0
        ynaph = ynaph*mass
    else:
        ynaph_mass = ynaph*mass
    ynaph_list.append(ynaph)
    naph_list_mass.append(ynaph_mass)

    ybenz = sum_liq*0.6
    if ybenz <0:
        ybenz = 0
        ybenz_mass = ybenz*mass
    else:
        ybenz_mass = ybenz*mass
    ybenz_list.append(ybenz)
    benz_list_mass.append(ybenz_mass)

    ytol = sum_liq*0.2
    if ytol <0:
        ytol = 0
        ytol_mass = ytol*mass
    else:
        ytol_mass = ytol*mass
    ytol_list.append(ytol)
    tol_list_mass.append(ytol_mass)
```

```
#Gases


ych4_list =[]
ch4_list_mass = []
yo2_list =[]
o2_list_mass = []
yco_list = []
co_list_mass = []
yco2_list = []
co2_list_mass = []
yh2_list = []
h2_list_mass = []

for i in range(0,n):
        sum_gas = ygases[i]*volatiles[i]

        yco =sum_gas*((-2.65*(temp_list[i])**2)*10**(-4)+0.27*(temp_list[i])-32.71)/100
        if yco < 0:
            yco = 0
            yco_mass = yco*mass
        else:
            yco_mass = yco*mass
        yco_list.append(yco)
        co_list_mass.append(yco_mass)

        yco2 = sum_gas*((-2.85*(temp_list[i])**2)*10**(-5)-0.029*(temp_list[i])+70.89)/100
        if yco2 < 0:
            yco2 = 0
            yco2_mass = yco2*mass
        else:
            yco2_mass = yco2*mass
        yco2_list.append(yco2)
        co2_list_mass.append(yco2_mass)


        ych4 = sum_gas*((6.69*(temp_list[i])**2)*10**(-5)-0.037*temp_list[i]+4.28)/100
        if ych4 < 0:
            ych4 = 0
            ych4_mass = ych4*mass
        else:
            ych4_mass = ych4*mass
        ych4_list.append(ych4)
        ch4_list_mass.append(ych4_mass)

        yh2 = sum_gas*((7*(temp_list[i])**2)*10**(-5)-0.0371*(temp_list[i])+5.11)/100
        if yh2 < 0:
            yh2 = 0
            yh2_mass = yh2* mass
        else:
            yh2_mass = yh2* mass
        yh2_list.append(yh2)
        h2_list_mass.append(yh2_mass)
```

```
#concentration of char
char = []
char_mass = []
for i in range(len(yC1_plot)):
        sum_char = yC1_plot[i]+yC2_plot[i] # charcoal fraction mass balance
        mass_sum_char = sum_char*mass # charcoal mass balance
        char_mass.append(mass_sum_char)
        char.append(sum_char)
```

```
#concentration of non-reacted and ash
residue = []
residue_mass = []
for i in range(len(yG1_plot)):
        sum_re = 1 - volatiles[i] - char[i] #residue fraction mass balance
        mass_sum_re = mass*sum_re #residue mass balance
        residue_mass.append(mass_sum_re)
        residue.append(sum_re)
```

```
plt.plot(xCB_plot,yCB_plot, label = "C. Biomass")
plt.plot(xG1_plot, volatiles, label = "C. Volatiles")
plt.plot(xC1_plot, char, label = "C. Charcoal")
plt.plot(xC1_plot, residue, label = "C. Unreacted")
plt.ylabel("Concentration")
plt.xlabel("time (s)")
plt.title(title)
plt.legend()
plt.show()
```

```
#carbon balance
#biomass = char + gases + liquids + residue

benz_mol_list = []
tol_mol_list = []
naph_mol_list = []

co_mol_list = []
co2_mol_list =[]
ch4_mol_list = []
h2_mol_list = []

ychar_mass_list_c = []
char_mol_list_c = []
char_mass_list_c = []
char_mol_list_s = []
char_mass_list_s = []

yresidue_list = []
water_list = []
sulfur_list = []

for i in range(0,n):

    #liquids
    mol_liquids_benz = benz_list_mass[i]/benz_mm*100
    mol_liquids_tol = tol_list_mass[i]/tol_mm*100
    mol_liquids_naph = naph_list_mass[i]/naph_mm*100
    benz_mol_list.append(mol_liquids_benz)
    naph_mol_list.append(mol_liquids_naph)
    tol_mol_list.append(mol_liquids_tol)

    #gases
    mol_gases_co = co_list_mass[i]/co_mm*100
    mol_gases_co2 = co2_list_mass[i]/co2_mm*100
    mol_gases_ch4 = ch4_list_mass[i]/ch4_mm*100
    mol_gases_h2 = h2_list_mass[i]/h2_mm*100
    co_mol_list.append(mol_gases_co)
    co2_mol_list.append(mol_gases_co2)
    ch4_mol_list.append(mol_gases_ch4)
    h2_mol_list.append(mol_gases_h2)

    #char carbon balance
    mol_char_c = char[i]*(c_mol_i - co_mol_list[i] - co2_mol_list[i] - ch4_mol_list[i] - benz_mol_list[i]*6 - tol_mol_list[i]*7-naph_mol_list[i]*10)
    char_mol_list_c.append(mol_char_c)
    mass_char_c = mol_char_c*c_mm/1000
    char_mass_list_c.append(mass_char_c)
    yc = mass_char_c/mass
    ychar_mass_list_c.append(yc)
    water_mass = water_mass_i/mass
    water_list.append(water_mass)
    sulfur_mass = s_mass_i/mass
    sulfur_list.append(sulfur_mass)
    yresidue = 1 -sulfur_list[i]-water_list[i]-yco_list[i] -yco2_list[i]-ych4_list[i]-yh2_list[i]-ybenz_list[i]-ytol_list[i]-ynaph_list[i]-ychar_mass_list_c[i]
    if yresidue<0:
        yresidue = 0
        yresidue_list.append(yresidue)
    else:
        yresidue_list.append(yresidue)
```

```
plt.plot(time_list,char_mass_list_c, label = "C(s)")
plt.plot(time_list,co_list_mass, label = "CO")
plt.plot(time_list,co2_list_mass, label = "CO2")
plt.plot(time_list,ch4_list_mass, label = "CH4")
plt.plot(time_list,h2_list_mass, label = "H2")
plt.plot(time_list,benz_list_mass, label = "Benzene")
plt.plot(time_list,tol_list_mass, label = "Toluene")
plt.plot(time_list,naph_list_mass, label = "Naphtalene")
plt.xlabel("Time (s)")
plt.ylabel("Mass (Kg)")
plt.legend()
plt.show()
```

```
plt.plot(temp_list,char_mass_list_c, label = "C(s)")
plt.plot(temp_list,co_list_mass, label = "CO")
plt.plot(temp_list,co2_list_mass, label = "CO2")
plt.plot(temp_list,ch4_list_mass, label = "CH4")
plt.plot(temp_list,h2_list_mass, label = "H2")
plt.plot(temp_list,benz_list_mass, label = "Benzene")
plt.plot(temp_list,tol_list_mass, label = "Toluene")
plt.plot(temp_list,naph_list_mass, label = "Naphtalene")
plt.xlabel("Temperature (K)")
plt.ylabel("Mass (Kg)")
plt.legend()
plt.show()
```

```
plt.plot(time_list,temp_list)
plt.ylabel("Temperature (K)")
plt.xlabel("Time (s)")

plt.show()
```

```
import pandas as pd

general_frac = pd.DataFrame(
    data = zip(time_list,temp_list,yco_list,yco2_list,ych4_list,yh2_list,ybenz_list,ytol_list,ynaph_list,ychar_mass_list_c,water_list,sulfur_list,yresidue_list),
    columns = ['Time (s)','Temp (K)','yCO','yCO2','yCH4','yH2','yBenz','yTol','yNaph','yC(s)','yWater','yS(s)','yUnreacted']
    )
print(general_frac)
```

```
plt.plot(time_list,yco_list, label = "yCO")
plt.plot(time_list,yco2_list, label = "yCO2")
plt.plot(time_list,ych4_list, label = "yCH4")
plt.plot(time_list,yh2_list, label = "yH2")
plt.plot(time_list,ybenz_list, label = "yBenzene")
plt.plot(time_list,ytol_list, label = "yToluene")
plt.plot(time_list,ynaph_list, label = "yNaphtalene")
plt.plot(time_list,ychar_mass_list_c, label = "yC(s)")
plt.plot(time_list, sulfur_list, label = "yS(s)")
plt.plot(time_list, water_list, label = "yWater")
plt.title(title)
plt.xlabel("Time (s)")
plt.ylabel("Mass fraction ")
plt.legend()
plt.show()
```